

## Supplementary Data

### Biotransformation of dehydroepiandrosterone (DHEA) by environmental strains of filamentous fungi

Ewa Kozłowska,<sup>\*a</sup> Monika Urbaniak,<sup>b</sup> Anna Kancelista,<sup>c</sup> Monika Dymarska,<sup>a</sup> Edyta Kostrzewska-Susłow,<sup>a</sup> Łukasz Stępień<sup>b</sup> and Tomasz Janeczko<sup>\*a</sup>

<sup>a</sup>Department of Chemistry, Wrocław University of Environmental and Life Sciences, Norwida 25, 50-375 Wrocław, Poland. E-mail: e.a.kozlowska@gmail.com; janeczko13@interia.pl

<sup>b</sup>Department of Pathogen Genetics and Plant Resistance, Institute of Plant Genetics, Polish Academy of Sciences, Strzeszyńska 34, 60-479 Poznań, Poland.

<sup>c</sup>Department of Biotechnology and Food Microbiology, Wrocław University of Environmental and Life Sciences, Chełmońskiego 37, 51-630 Wrocław, Poland.

\*Corresponding author: E-mail: e.a.kozlowska@gmail.com (Ewa Kozłowska); janeczko13@interia.pl (Tomasz Janeczko)

### Content

Table S1. <sup>13</sup>C NMR chemical shifts of products in CDCl<sub>3</sub> (recorded in CDCl<sub>3</sub> 113 MHz)

Fig.S1. <sup>1</sup>H NMR spectral of androst-1,4-diene-3,17-dione (**ADD**) (CDCl<sub>3</sub>, 600 MHz)

Fig.S2. <sup>13</sup>C NMR spectral of androst-1,4-diene-3,17-dione (**ADD**) (CDCl<sub>3</sub>, 151 MHz)

Fig.S3. HSQC spectral of androst-1,4-diene-3,17-dione (**ADD**) (CDCl<sub>3</sub>, 151 MHz)

Fig.S4. COSY spectral of androst-1,4-diene-3,17-dione (**ADD**) (CDCl<sub>3</sub>, 151 MHz)

Fig.S5. <sup>1</sup>H NMR spectral of 6 $\beta$ -hydroxyandrost-4-ene-3,17-dione (**6 $\beta$ OH-AD**) (CDCl<sub>3</sub>, 600 MHz)

Fig.S6. <sup>13</sup>C NMR spectral of 6 $\beta$ -hydroxyandrost-4-ene-3,17-dione (**6 $\beta$ OH-AD**) (CDCl<sub>3</sub>, 151 MHz)

Fig.S7. HSQC spectral of 6 $\beta$ -hydroxyandrost-4-ene-3,17-dione (**6 $\beta$ OH-AD**) (CDCl<sub>3</sub>, 151 MHz)

Fig.S8. COSY spectral of 6 $\beta$ -hydroxyandrost-4-ene-3,17-dione (**6 $\beta$ OH-AD**) (CDCl<sub>3</sub>, 151 MHz)

Fig.S9. <sup>1</sup>H NMR spectral of 6 $\beta$ -hydroxyandrost-1,4-diene-3,17-dione (**6 $\beta$ OH-ADD**) (CDCl<sub>3</sub>, 600 MHz)

Fig.S10. <sup>13</sup>C NMR spectral of 6 $\beta$ -hydroxyandrost-1,4-diene-3,17-dione (**6 $\beta$ OH-ADD**) (CDCl<sub>3</sub>, 151 MHz)

Fig.S11. HSQC spectral of 6 $\beta$ -hydroxyandrost-1,4-diene-3,17-dione (**6 $\beta$ OH-ADD**) (CDCl<sub>3</sub>, 151 MHz)

- Fig.S12. COSY spectral of 6 $\beta$ -hydroxyandrost-1,4-diene-3,17-dione (**6 $\beta$ OH-ADD**) (CDCl<sub>3</sub>, 151 MHz)
- Fig.S13. <sup>1</sup>H NMR spectral of 3 $\beta$ -hydroxy-17a-oxa-D-homo-androst-5-ene-17-one (**3 $\beta$ OH-lactone**) (CDCl<sub>3</sub>, 600 MHz)
- Fig.S14. <sup>13</sup>C NMR spectral of 3 $\beta$ -hydroxy-17a-oxa-D-homo-androst-5-ene-17-one (**3 $\beta$ OH-lactone**) (CDCl<sub>3</sub>, 151 MHz)
- Fig.S15. HSQC spectral of 3 $\beta$ -hydroxy-17a-oxa-D-homo-androst-5-ene-17-one (**3 $\beta$ OH-lactone**) (CDCl<sub>3</sub>, 151 MHz)
- Fig.S16. COSY spectral of 3 $\beta$ -hydroxy-17a-oxa-D-homo-androst-5-ene-17-one (**3 $\beta$ OH-lactone**) (CDCl<sub>3</sub>, 151 MHz)
- Fig.S17. <sup>1</sup>H NMR spectral of 17a-oxa-D-homo-androst-4-ene-17-one (**testololactone**) (CDCl<sub>3</sub>, 600 MHz)
- Fig.S18. <sup>13</sup>C NMR spectral of 17a-oxa-D-homo-androst-4-ene-17-one (**testololactone**) (CDCl<sub>3</sub>, 151 MHz)
- Fig.S19. HSQC spectral of 17a-oxa-D-homo-androst-4-ene-17-one (**testololactone**) (CDCl<sub>3</sub>, 151 MHz)
- Fig.S20. COSY spectral of 17a-oxa-D-homo-androst-4-ene-17-one (**testololactone**) (CDCl<sub>3</sub>, 151 MHz)
- Fig.S21. <sup>1</sup>H NMR spectral of 3 $\beta$ ,7 $\alpha$ -dihydroxyandrost-5-ene-17-one (**7 $\alpha$ OH-DHEA**) (CDCl<sub>3</sub>, 600 MHz)
- Fig.S22. <sup>13</sup>C NMR spectral of 3 $\beta$ ,7 $\alpha$ -dihydroxyandrost-5-ene-17-one (**7 $\alpha$ OH-DHEA**) (CDCl<sub>3</sub>, 151 MHz)
- Fig.S23. HSQC spectral of 3 $\beta$ ,7 $\alpha$ -dihydroxyandrost-5-ene-17-one (**7 $\alpha$ OH-DHEA**) (CDCl<sub>3</sub>, 151 MHz)
- Fig.S24. COSY spectral of 3 $\beta$ ,7 $\alpha$ -dihydroxyandrost-5-ene-17-one (**7 $\alpha$ OH-DHEA**) (CDCl<sub>3</sub>, 151 MHz)
- Fig.S25. <sup>1</sup>H NMR spectral of androst-5-ene-3 $\beta$ ,7 $\alpha$ ,17 $\alpha$ -triol (**3 $\beta$ ,7 $\alpha$ ,17 $\alpha$ -triol**) (CDCl<sub>3</sub>, 600 MHz)
- Fig.S26. <sup>13</sup>C NMR spectral of androst-5-ene-3 $\beta$ ,7 $\alpha$ ,17 $\alpha$ -triol (**3 $\beta$ ,7 $\alpha$ ,17 $\alpha$ -triol**) (CDCl<sub>3</sub>, 151 MHz)
- Fig.S27. HSQC spectral of androst-5-ene-3 $\beta$ ,7 $\alpha$ ,17 $\alpha$ -triol (**3 $\beta$ ,7 $\alpha$ ,17 $\alpha$ -triol**) (CDCl<sub>3</sub>, 151 MHz)
- Fig.S28. COSY spectral of androst-5-ene-3 $\beta$ ,7 $\alpha$ ,17 $\alpha$ -triol (**3 $\beta$ ,7 $\alpha$ ,17 $\alpha$ -triol**) (CDCl<sub>3</sub>, 151 MHz)
- Fig.S29. <sup>1</sup>H NMR spectral of 3 $\beta$ -hydroxyandrost-5-ene-7,17-dione (**7Oxo-DHEA**) (CDCl<sub>3</sub>, 600 MHz)
- Fig.S30. <sup>13</sup>C NMR spectral of 3 $\beta$ -hydroxyandrost-5-ene-7,17-dione (**7Oxo-DHEA**) (CDCl<sub>3</sub>, 151 MHz)
- Fig.S31. HSQC spectral of 3 $\beta$ -hydroxyandrost-5-ene-7,17-dione (**7Oxo-DHEA**) (CDCl<sub>3</sub>, 151 MHz)
- Fig.S32. COSY spectral of 3 $\beta$ -hydroxyandrost-5-ene-7,17-dione (**7Oxo-DHEA**) (CDCl<sub>3</sub>, 151 MHz)

Table S2. Intensity of fragments arising from degradation of compound androst-1,4-diene-3,17-dione (**ADD**)

Fig.S33. GC-MS spectra of androst-1,4-diene-3,17-dione (**ADD**)

Fig.S34. Enlarged GC-MS spectra of androst-1,4-diene-3,17-dione (**ADD**)

Table S3. Intensity of fragments arising from degradation of compound 6 $\beta$ -hydroxyandrost-4-ene-3,17-dione (**6 $\beta$ OH-AD**)

Fig.S35. GC-MS spectra of 6 $\beta$ -hydroxyandrost-4-ene-3,17-dione (**6 $\beta$ OH-AD**)

Fig.S36. Enlarged GC-MS spectra of 6 $\beta$ -hydroxyandrost-4-ene-3,17-dione (**6 $\beta$ OH-AD**)

Table S4. Intensity of fragments arising from degradation of compound 6 $\beta$ -hydroxyandrost-1,4-diene-3,17-dione (**6 $\beta$ OH-ADD**)

Fig.S37. GC-MS spectra of 6 $\beta$ -hydroxyandrost-1,4-diene-3,17-dione (**6 $\beta$ OH-ADD**)

Fig.S38. Enlarged GC-MS spectra of 6 $\beta$ -hydroxyandrost-1,4-diene-3,17-dione (**6 $\beta$ OH-ADD**)

Table S5. Intensity of fragments arising from degradation of compound 3 $\beta$ -hydroxy-17a-oxa-D-homo-androst-5-ene-17-one (**3 $\beta$ OH-lactone**)

Fig.S39. GC-MS spectra of 3 $\beta$ -hydroxy-17a-oxa-D-homo-androst-5-ene-17-one (**3 $\beta$ OH-lactone**)

Fig.S40. Enlarged GC-MS spectra of 3 $\beta$ -hydroxy-17a-oxa-D-homo-androst-5-ene-17-one (**3 $\beta$ OH-lactone**)

Table S6. Intensity of fragments arising from degradation of compound 17a-oxa-D-homo-androst-4-ene-17-one (**testololactone**)

Fig.S41. GC-MS spectra of 17a-oxa-D-homo-androst-4-ene-17-one (**testololactone**)

Fig.S42. Enlarged GC-MS spectra of 17a-oxa-D-homo-androst-4-ene-17-one (**testololactone**)

Table S7. Intensity of fragments arising from degradation of compound 3 $\beta$ ,7 $\alpha$ -dihydroxyandrost-5-ene-17-one (**7 $\alpha$ OH-DHEA**)

Fig.S43. GC-MS spectra of 3 $\beta$ ,7 $\alpha$ -dihydroxyandrost-5-ene-17-one (**7 $\alpha$ OH-DHEA**)

Fig.S44. Enlarged GC-MS spectra of 3 $\beta$ ,7 $\alpha$ -dihydroxyandrost-5-ene-17-one (**7 $\alpha$ OH-DHEA**)

Table S8. Intensity of fragments arising from degradation of compound androst-5-ene-3 $\beta$ ,7 $\alpha$ ,17 $\alpha$ -triol (**3 $\beta$ ,7 $\alpha$ ,17 $\alpha$ -triol**)

Fig.S45. GC-MS spectra of androst-5-ene-3 $\beta$ ,7 $\alpha$ ,17 $\alpha$ -triol (**3 $\beta$ ,7 $\alpha$ ,17 $\alpha$ -triol**)

Fig.S46. Enlarged GC-MS spectra of androst-5-ene-3 $\beta$ ,7 $\alpha$ ,17 $\alpha$ -triol (**3 $\beta$ ,7 $\alpha$ ,17 $\alpha$ -triol**)

Table S9. Intensity of fragments arising from degradation of compound 3 $\beta$ -hydroxyandrost-5-ene-7,17-dione (**7Oxo-DHEA**)

Fig.S47. GC-MS spectra of 3 $\beta$ -hydroxyandrost-5-ene-7,17-dione (**7Oxo-DHEA**)

Fig.S48. Enlarged GC-MS spectra of 3 $\beta$ -hydroxyandrost-5-ene-7,17-dione (**7Oxo-DHEA**)

Table S1.  $^{13}\text{C}$  NMR chemical shifts of products in  $\text{CDCl}_3$ 

Atom numbe r	Products								
	<b>AD</b>	<b>ADD</b>	<b><math>6\beta\text{OH-}</math> AD</b>	<b><math>6\beta\text{OH-}</math> ADD</b>	<b>Testolo -lactone</b>	<b><math>7\alpha\text{OH-}</math> DHEA</b>	<b><math>3\beta,7\alpha,1</math> <math>7\alpha</math>-triol</b>	<b><math>3\beta\text{OH-}</math> lactone</b>	<b><math>7\text{Oxo-}</math> DHEA</b>
1	35.05	155.43	37.34	156.86	35.46	37.07	37.22	37.04	36.60
2	33.81	127.82	34.28	127.03	33.84	31.39	31.10	31.59	31.25
3	199.21	186.33	200.40	186.65	199.40	71.25	71.41	71.61	70.44
4	124.04	124.24	126.58	126.17	124.07	42.06	42.19	42.01	41.99
5	170.26	168.44	168.03	165.52	169.63	146.64	146.28	140.79	166.27
6	32.46	32.65	72.83	73.70	32.35	123.67	123.99	120.70	126.06
7	30.66	32.41	37.34	38.86	30.37	64.37	65.63	31.20	201.20
8	35.58	35.22	29.52	29.93	37.92	37.32	37.98	34.58	44.47
9	53.70	52.40	53.76	51.96	52.45	42.72	42.49	49.11	50.22
10	38.56	43.54	38.17	43.62	38.46	37.63	37.60	36.92	38.54
11	20.23	22.20	20.37	22.04	21.82	20.19	20.43	22.09	20.72
12	31.19	31.30	31.37	31.34	38.93	31.18	31.51	39.04	30.85
13	47.41	47.79	47.74	47.87	82.87	47.23	45.08	83.30	48.00
14	50.71	50.53	51.00	50.63	45.62	45.05	42.13	46.85	45.88
15	21.67	22.02	21.81	21.96	19.82	22.02	24.89	20.03	24.31
16	35.67	35.74	35.88	35.80	28.53	35.91	32.75	28.95	35.77
17	220.35	220.03	220.69	220.15	171.44	221.30	80.00	171.64	220.52
18	13.62	13.92	13.88	14.01	17.40	13.39	16.76	20.20	13.89
19	17.29	18.83	19.65	20.59	20.11	18.38	18.43	19.42	17.57

Fig.S1.  $^1\text{H}$  NMR spectral of androst-1,4-diene-3,17-dione (**ADD**) ( $\text{CDCl}_3$ , 600 MHz)

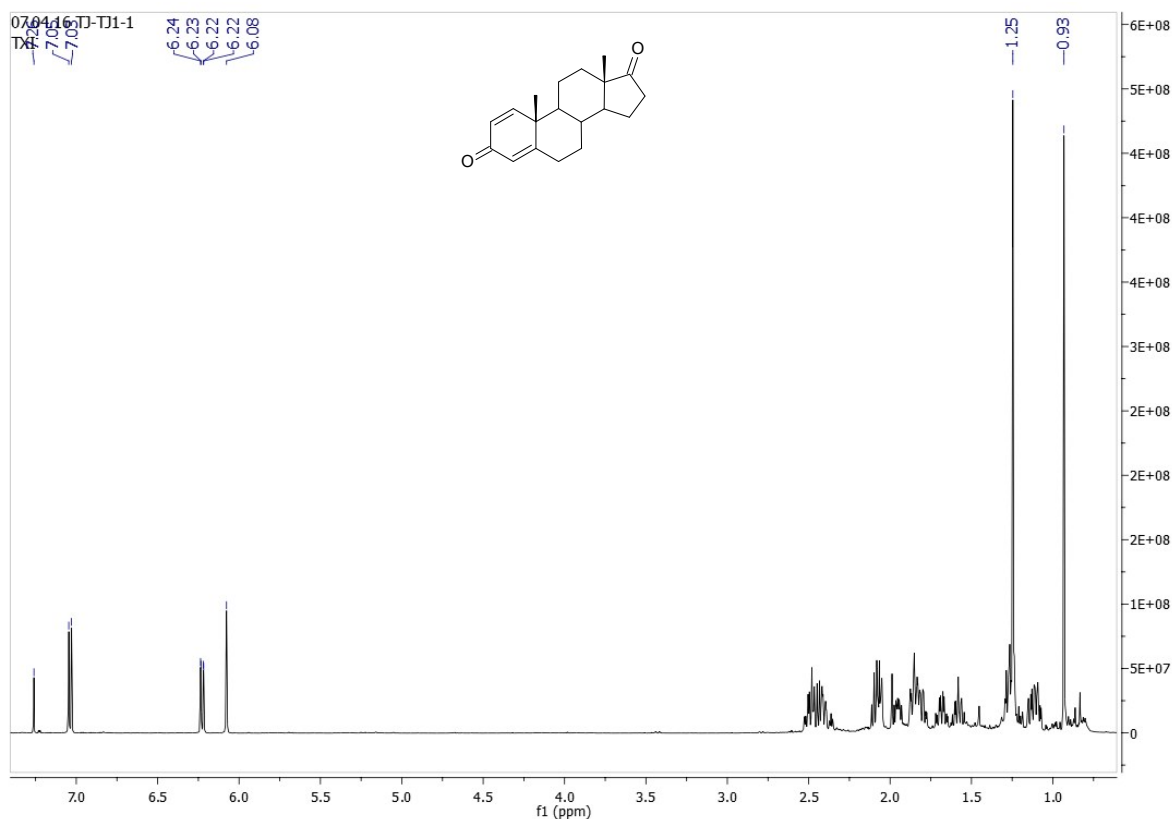


Fig.S2.  $^{13}\text{C}$  NMR spectral of androst-1,4-diene-3,17-dione (**ADD**) ( $\text{CDCl}_3$ , 151 MHz)

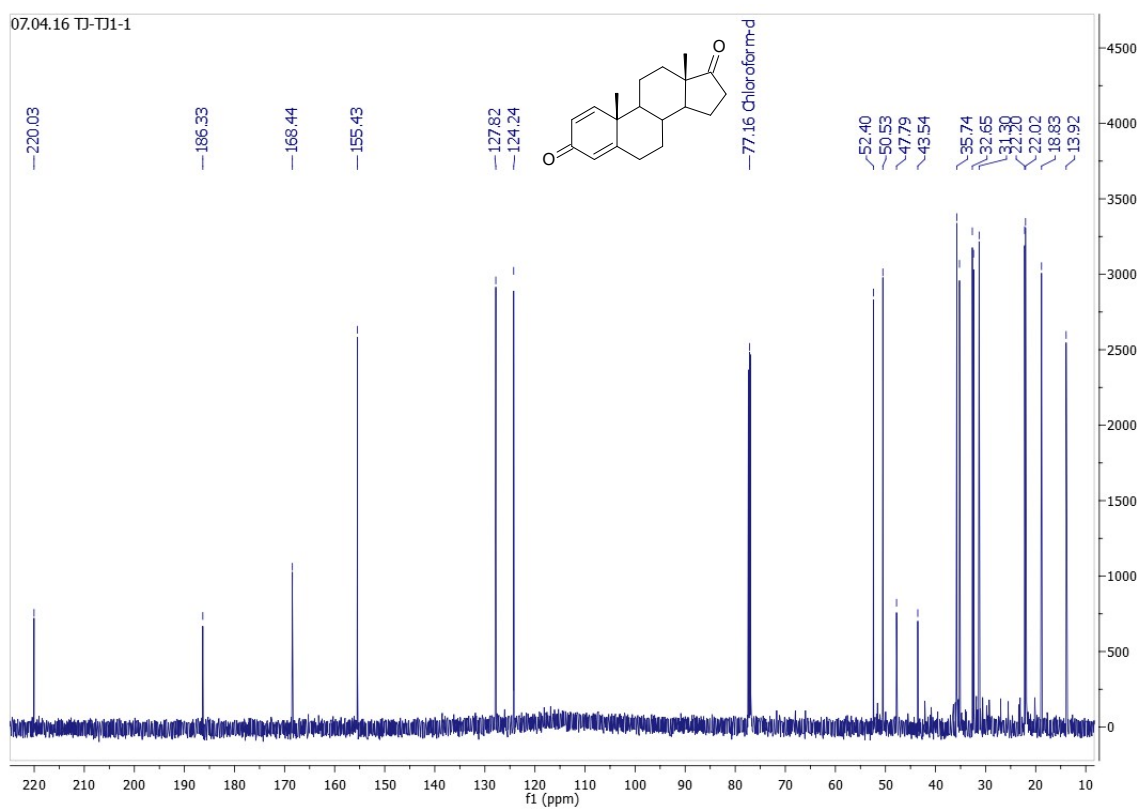


Fig.S3. HSQC spectral of androst-1,4-diene-3,17-dione (**ADD**) ( $\text{CDCl}_3$ , 151 MHz)

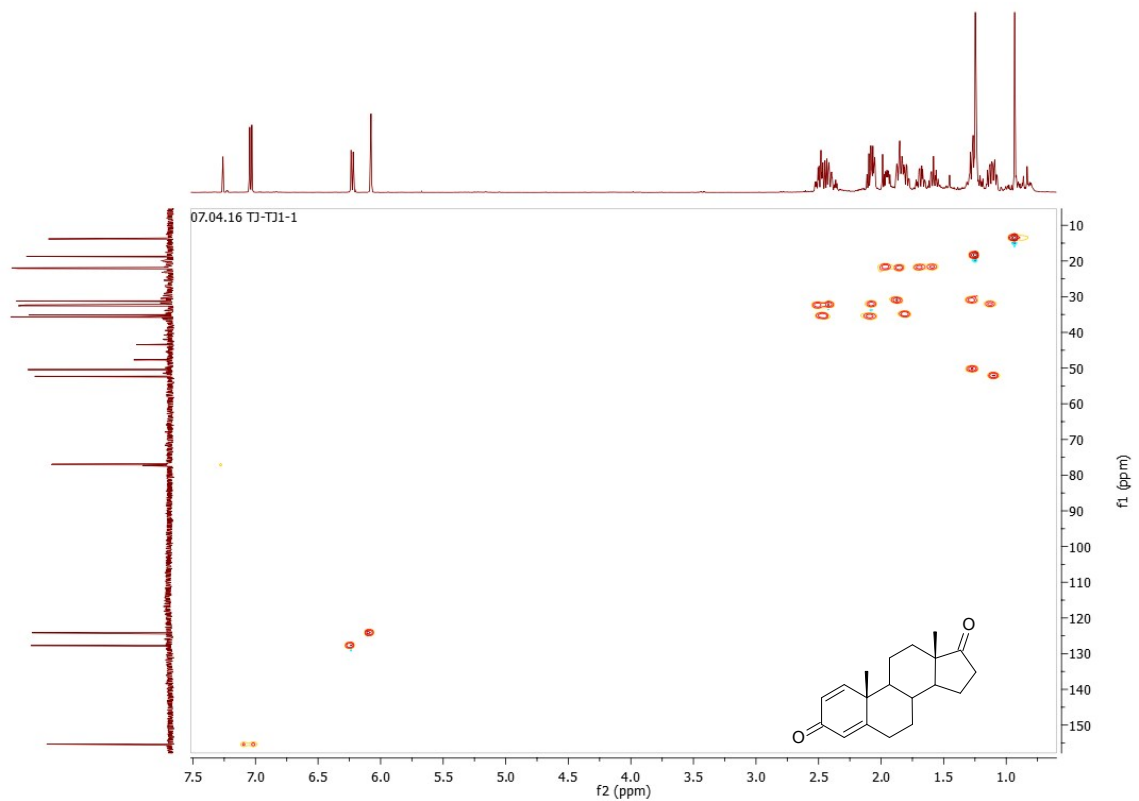


Fig.S4. COSY spectral of androst-1,4-diene-3,17-dione (**ADD**) ( $\text{CDCl}_3$ , 151 MHz)

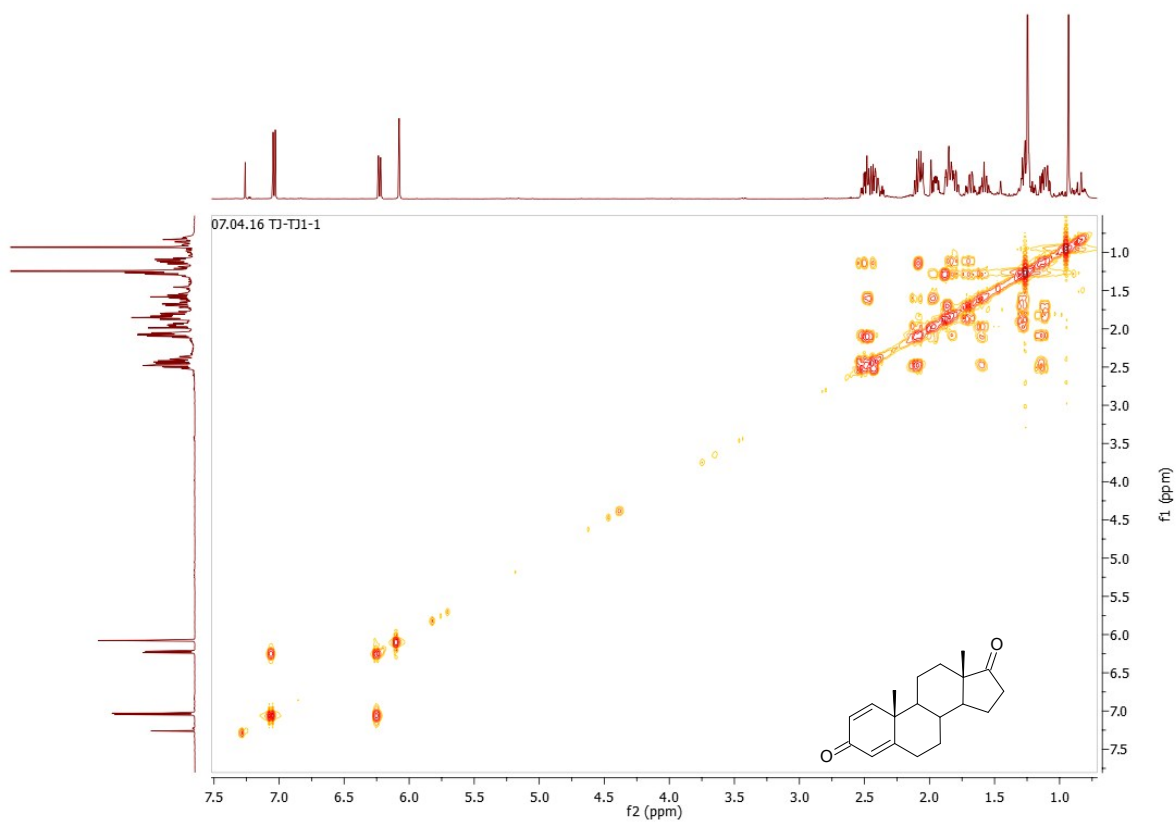


Fig.S5.  $^1\text{H}$  NMR spectral of  $6\beta$ -hydroxyandrost-4-ene-3,17-dione (**6 $\beta$ OH-AD**) ( $\text{CDCl}_3$ , 600 MHz)

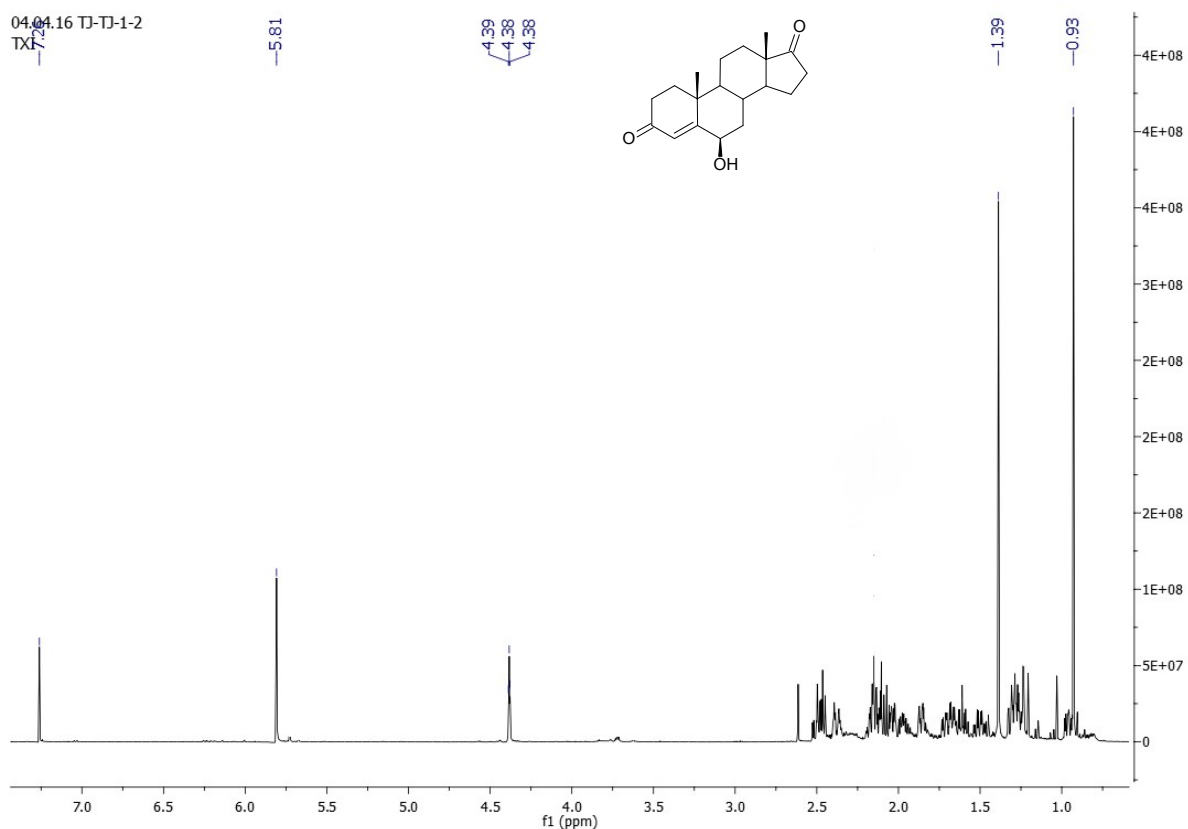


Fig.S6.  $^{13}\text{C}$  NMR spectral of  $6\beta$ -hydroxyandrost-4-ene-3,17-dione (**6 $\beta$ OH-AD**) ( $\text{CDCl}_3$ , 151 MHz)

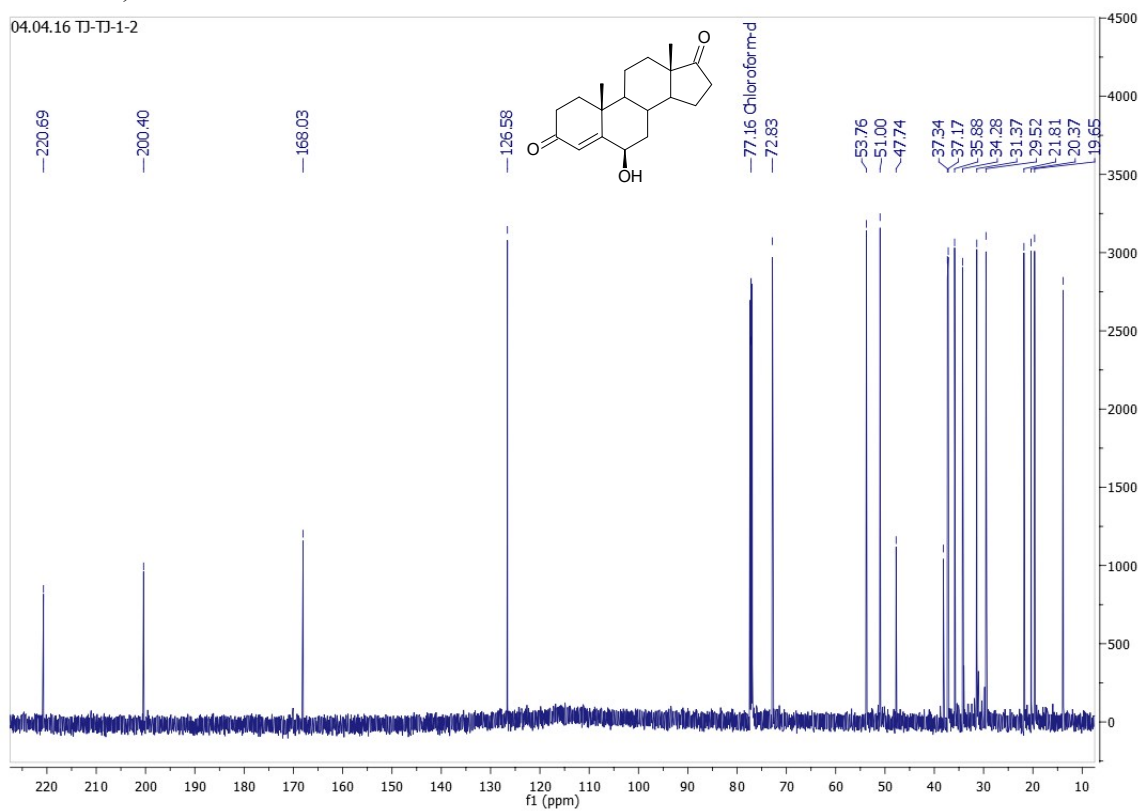


Fig.S7. HSQC spectral of 6 $\beta$ -hydro xyandrostan-4-ene-3,17-dione (**6 $\beta$ OH-AD**) ( $\text{CDCl}_3$ , 151 MHz)

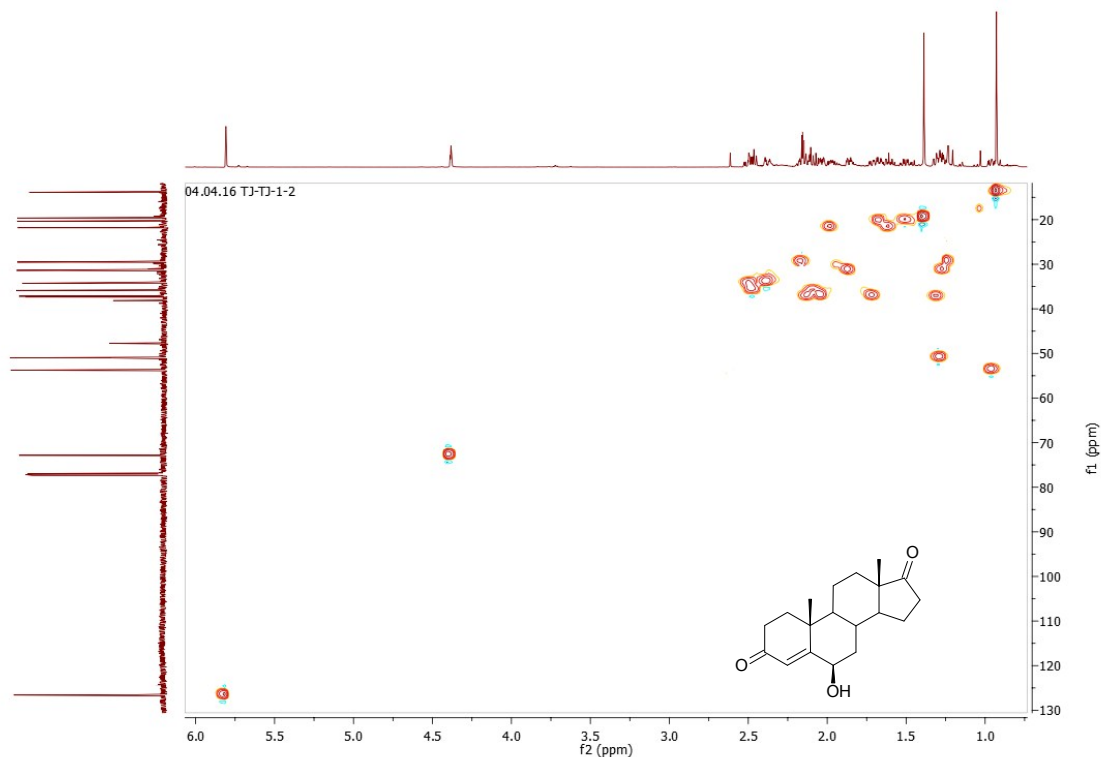


Fig.S8. COSY spectral of 6 $\beta$ -hydroxyxyandrostan-4-ene-3,17-dione (**6 $\beta$ OH-AD**) ( $\text{CDCl}_3$ , 151 MHz)

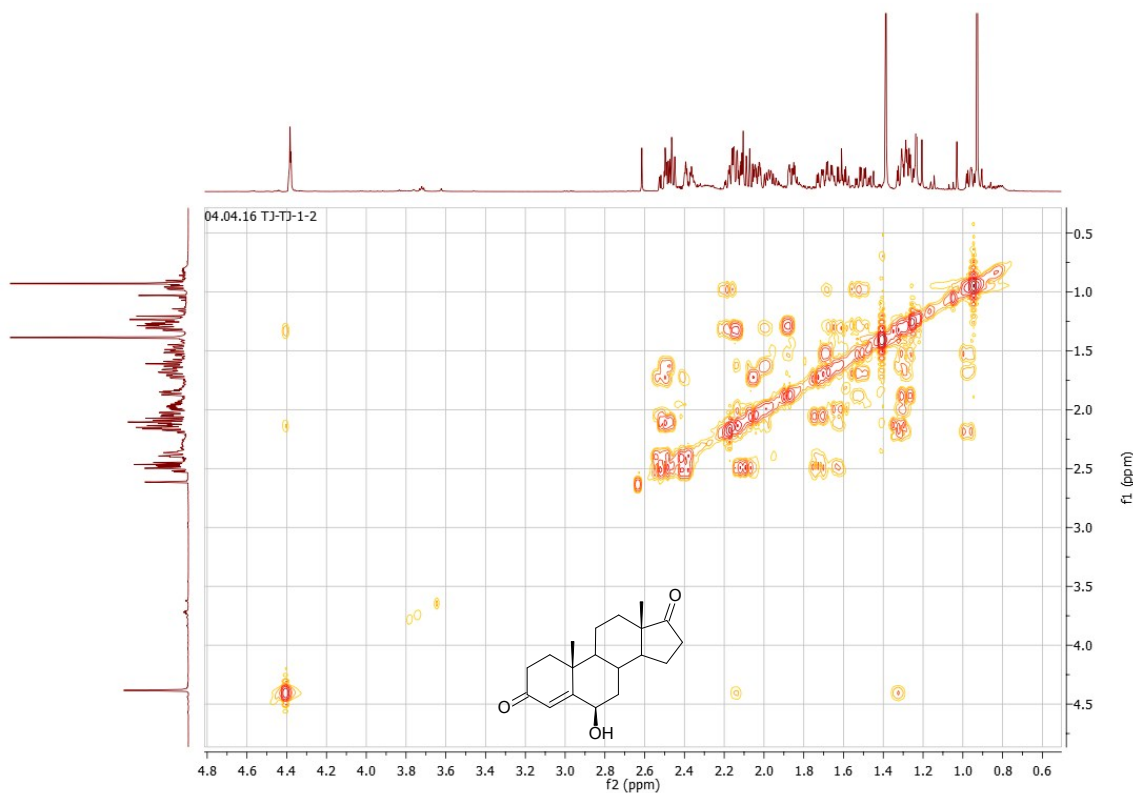


Fig.S9.  $^1\text{H}$  NMR spectral of 6 $\beta$ -hydroxyandrost-1,4-diene-3,17-dione (**6 $\beta$ OH-ADD**) ( $\text{CDCl}_3$ , 600 MHz)

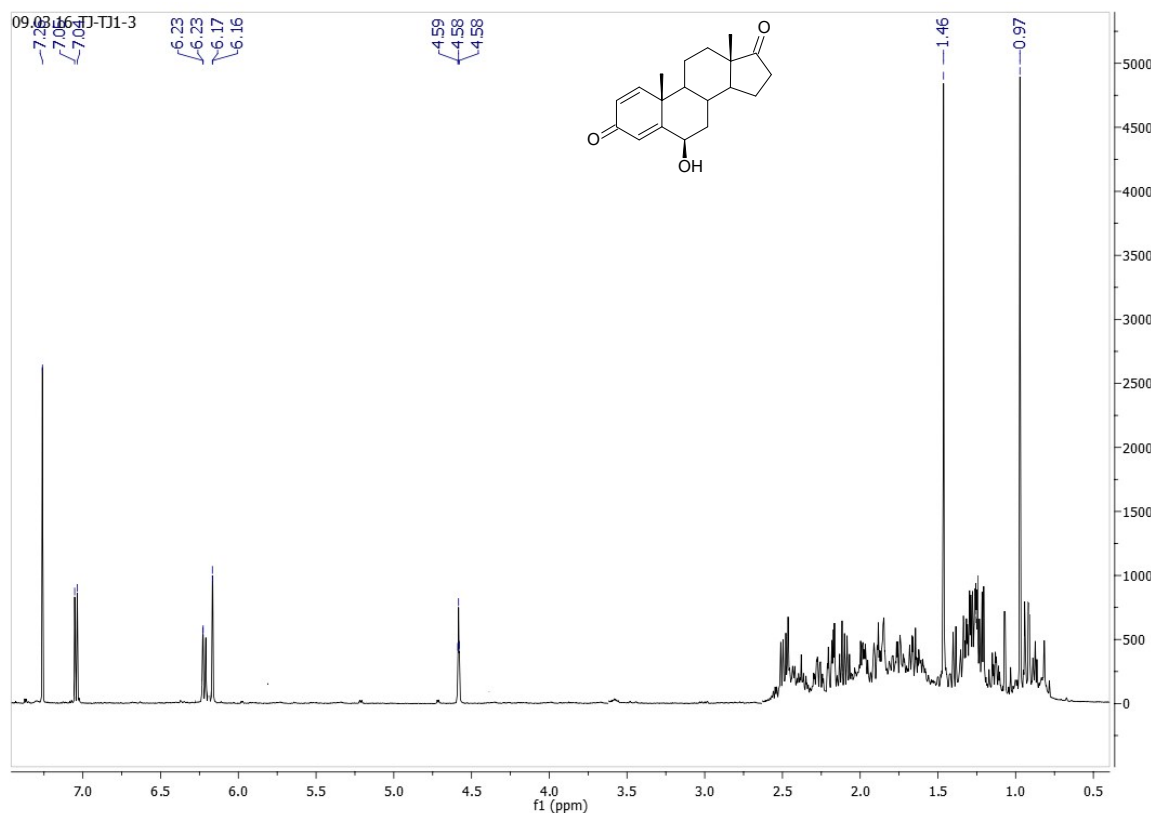


Fig.S10.  $^{13}\text{C}$  NMR spectral of 6 $\beta$ -hydroxyandrost-1,4-diene-3,17-dione (**6 $\beta$ OH-ADD**) ( $\text{CDCl}_3$ , 151 MHz)

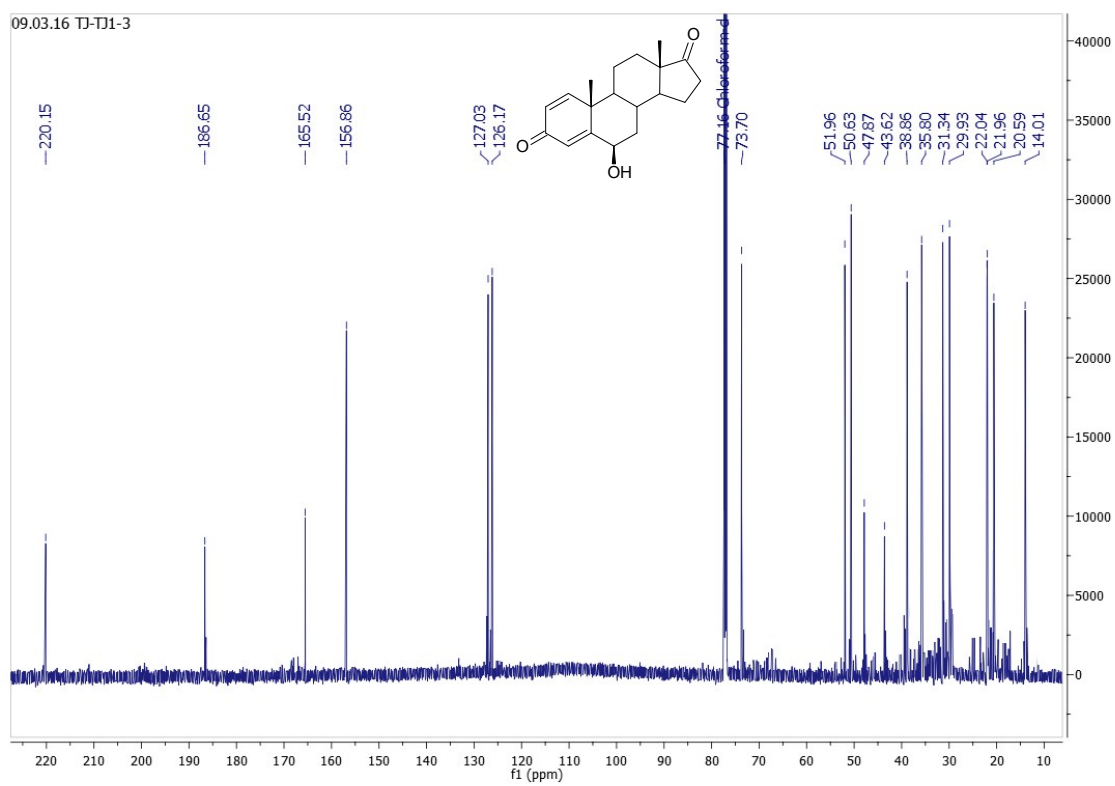


Fig.S11. HSQC spectral of  $6\beta$ -hydroxyandrost-1,4-diene-3,17-dione (**6 $\beta$ OH-ADD**) ( $\text{CDCl}_3$ , 151 MHz)

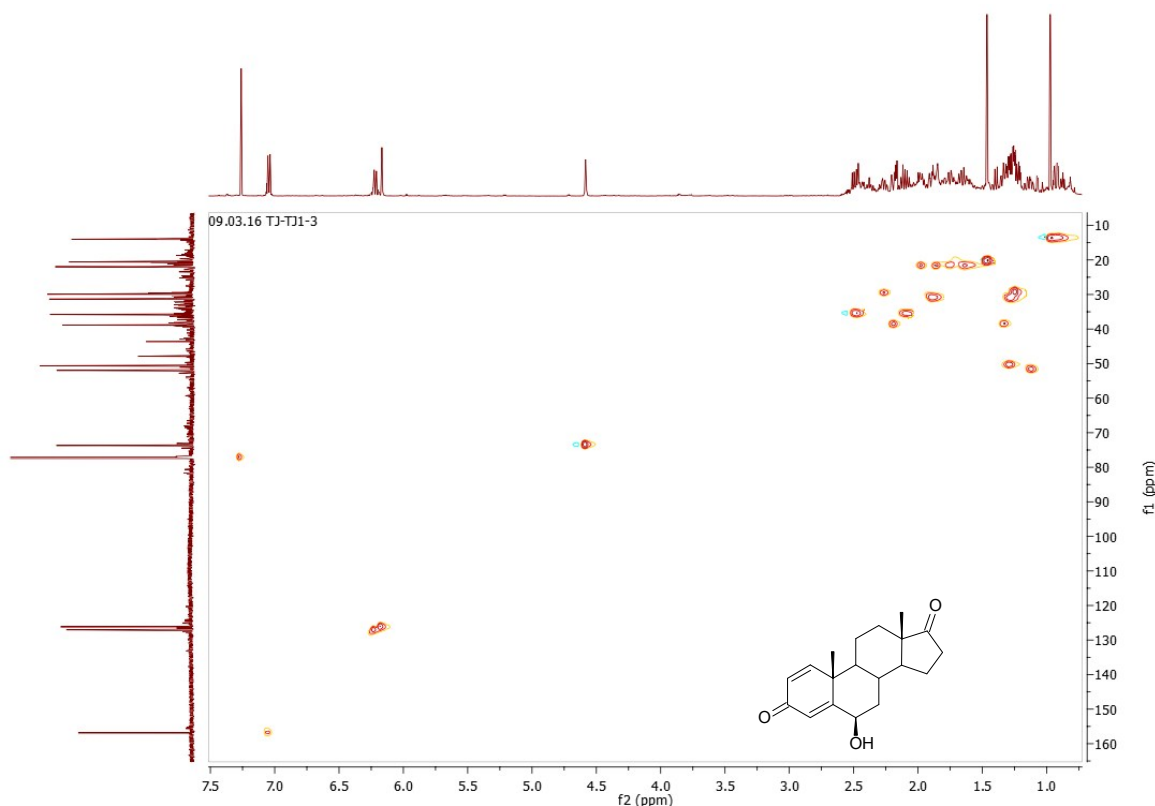


Fig.S12. COSY spectral of  $6\beta$ -hydroxyandrost-1,4-diene-3,17-dione (**6 $\beta$ OH-ADD**) ( $\text{CDCl}_3$ , 151 MHz)

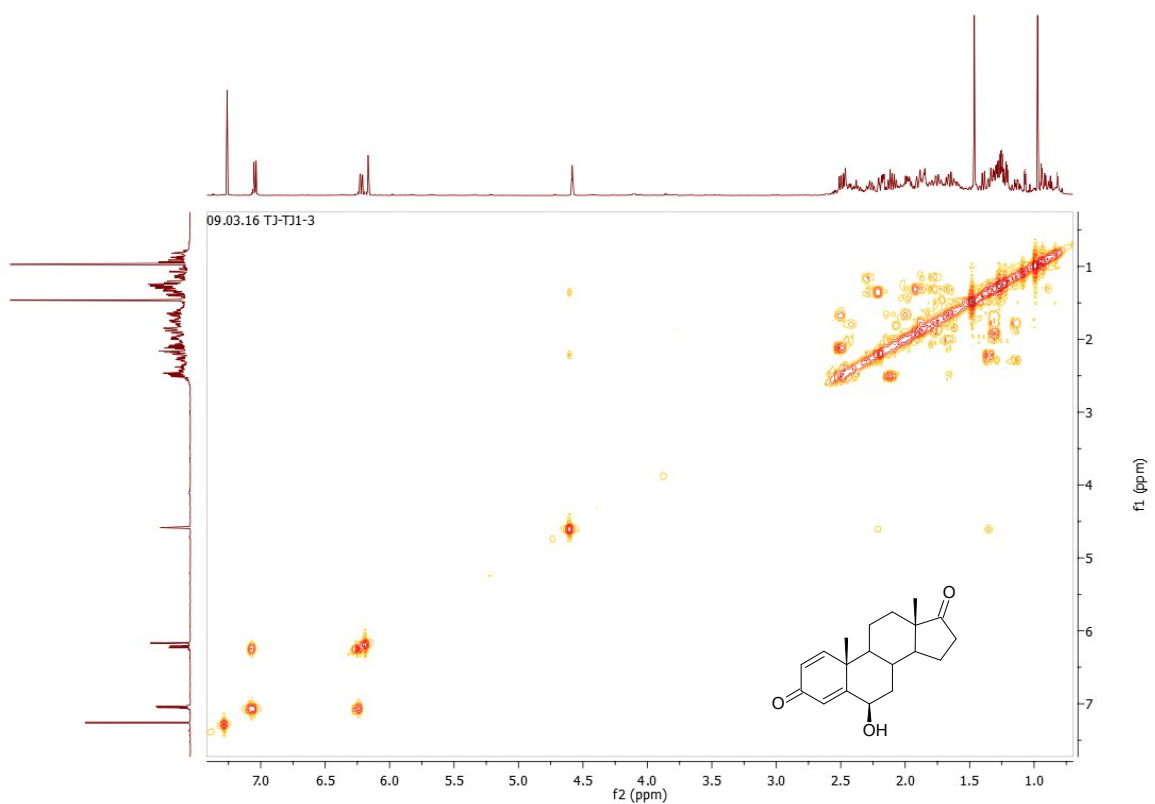


Fig.S13.  $^1\text{H}$  NMR spectral of 3 $\beta$ -hydroxy-17 $\alpha$ -oxa-D-homo-androst-5-ene-17-one (**3 $\beta$ OH-lactone**) ( $\text{CDCl}_3$ , 600 MHz)

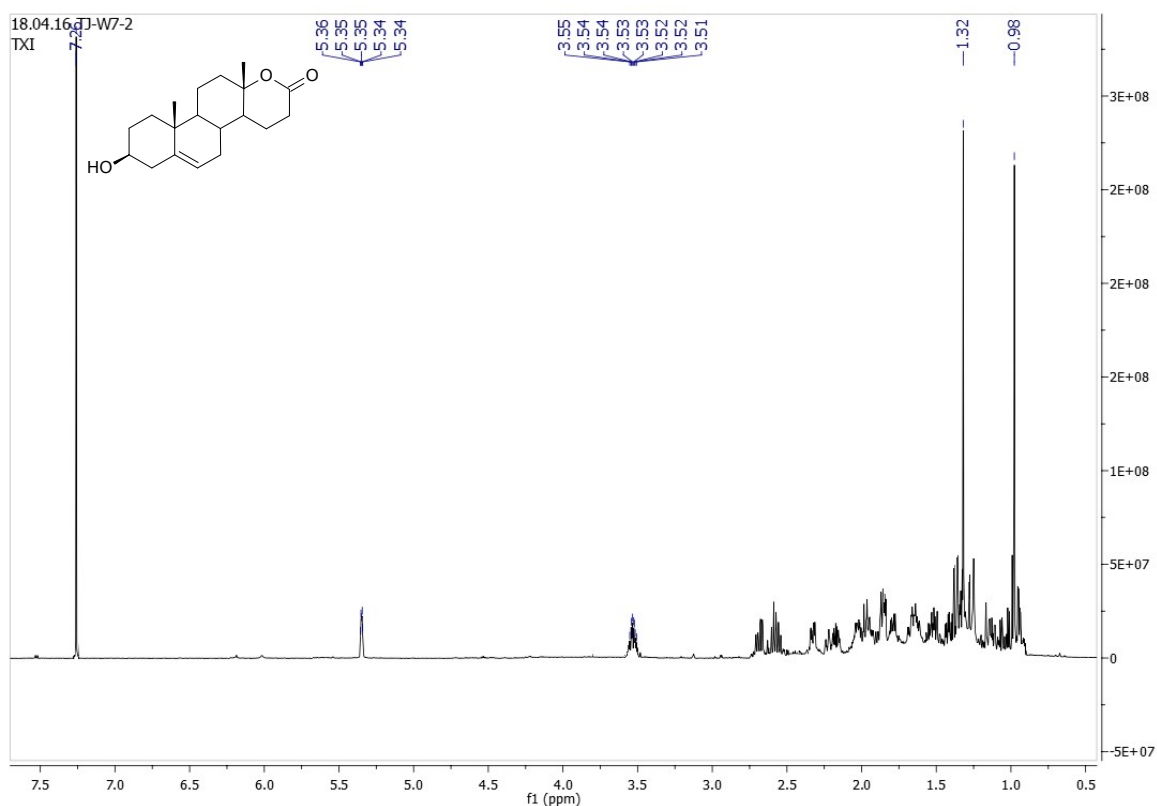


Fig.S14.  $^{13}\text{C}$  NMR spectral of 3 $\beta$ -hydroxy-17 $\alpha$ -oxa-D-homo-androst-5-ene-17-one (**3 $\beta$ OH-lactone**) ( $\text{CDCl}_3$ , 151 MHz)

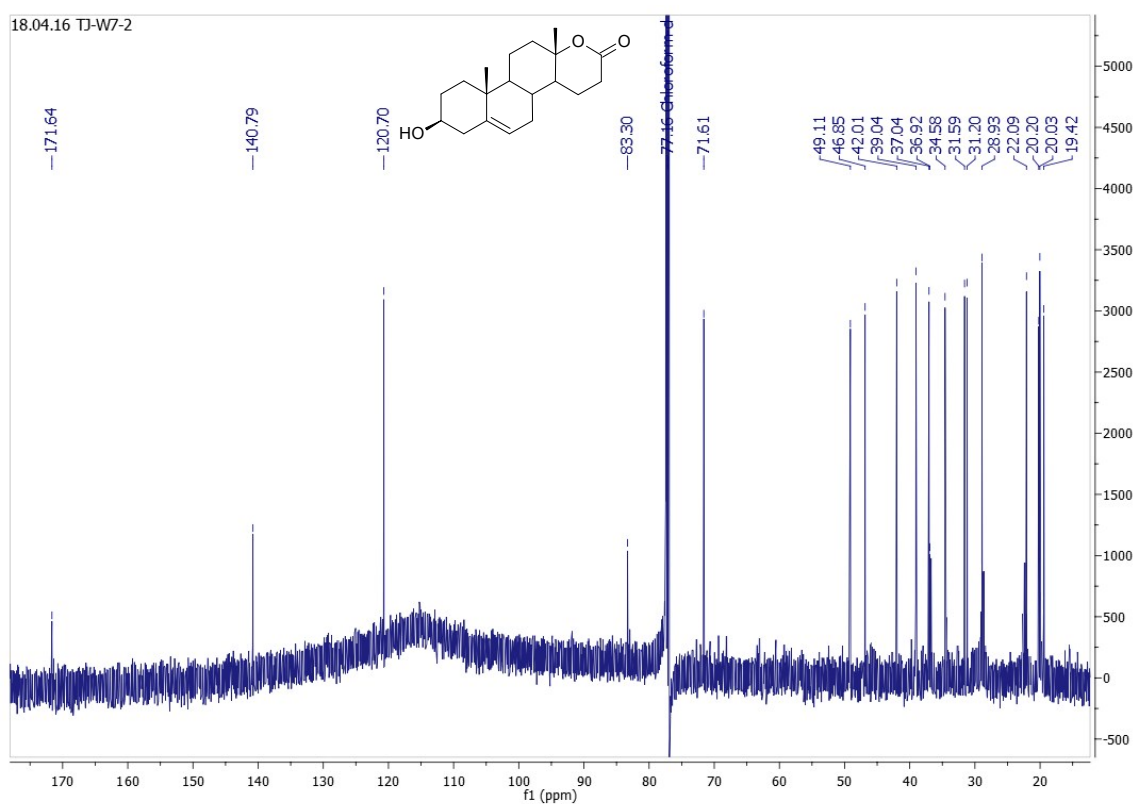


Fig.S15. HSQC spectral of 3 $\beta$ -hydroxy-17 $\alpha$ -oxa-D-homo-androst-5-ene-17-one (**3 $\beta$ OH-lactone**) ( $\text{CDCl}_3$ , 151 MHz)

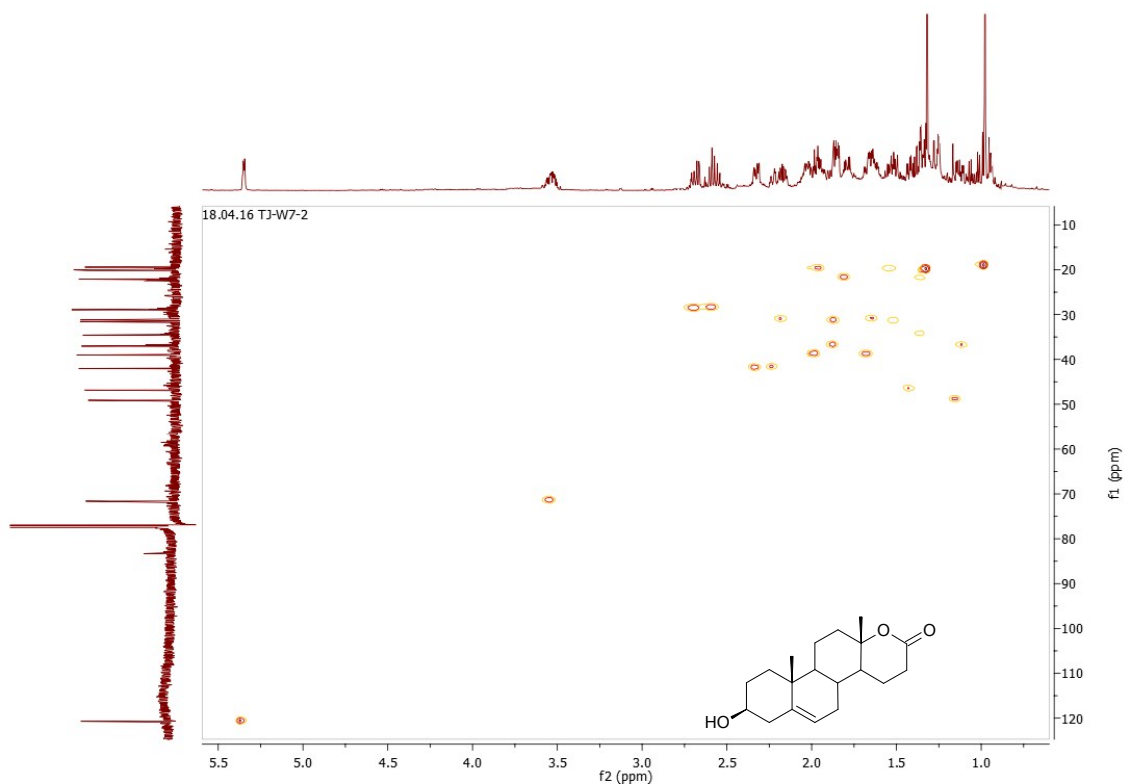


Fig.S16. COSY spectral of 3 $\beta$ -hydroxy-17 $\alpha$ -oxa-D-homo-androst-5-ene-17-one (**3 $\beta$ OH-lactone**) ( $\text{CDCl}_3$ , 151 MHz)

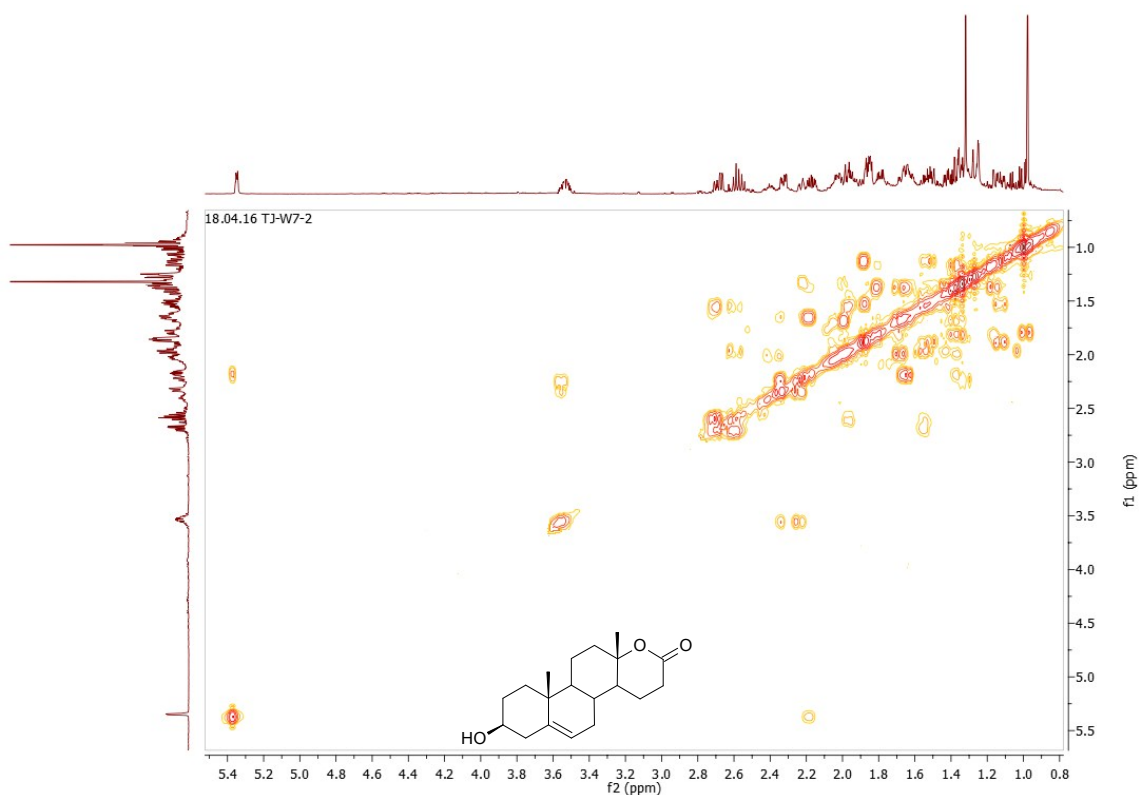


Fig.S17.  $^1\text{H}$  NMR spectral of 17a-oxa-D-homo-androst-4-ene-17-one (**testololactone**) ( $\text{CDCl}_3$ , 600 MHz)

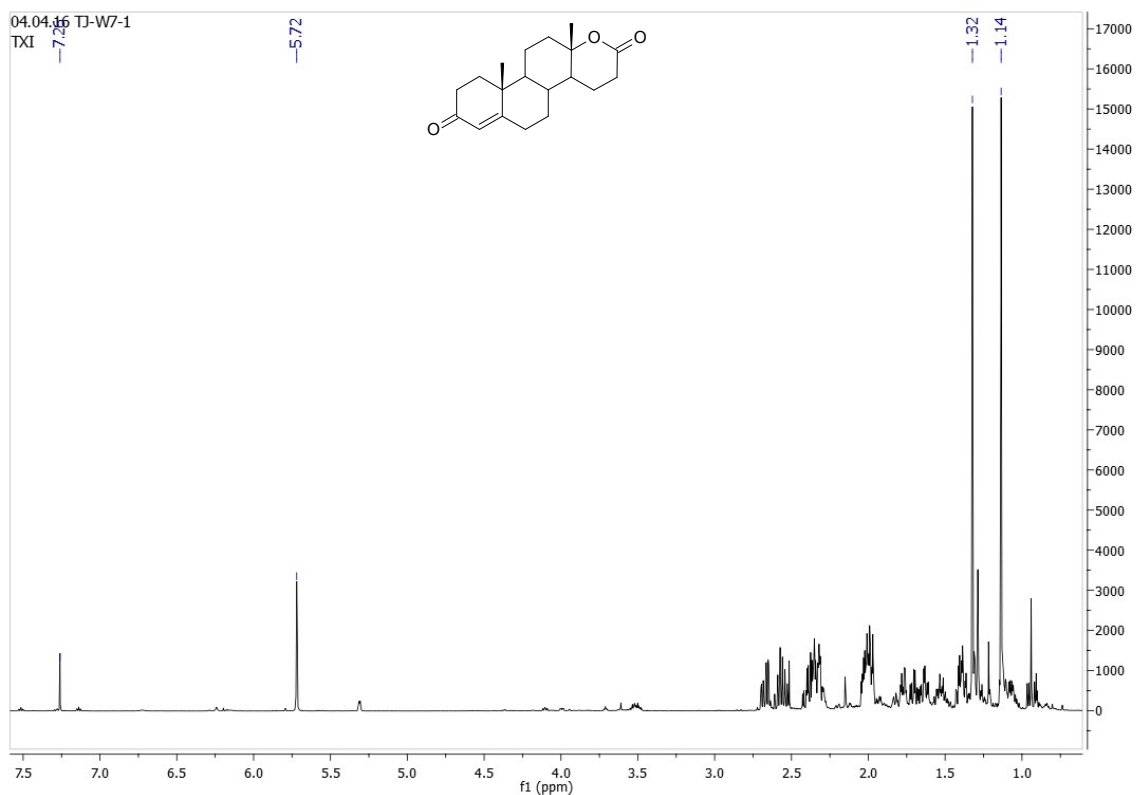


Fig.S18.  $^{13}\text{C}$  NMR spectral of 17a-oxa-D-homo-androst-4-ene-17-one (**testololactone**) ( $\text{CDCl}_3$ , 151 MHz)

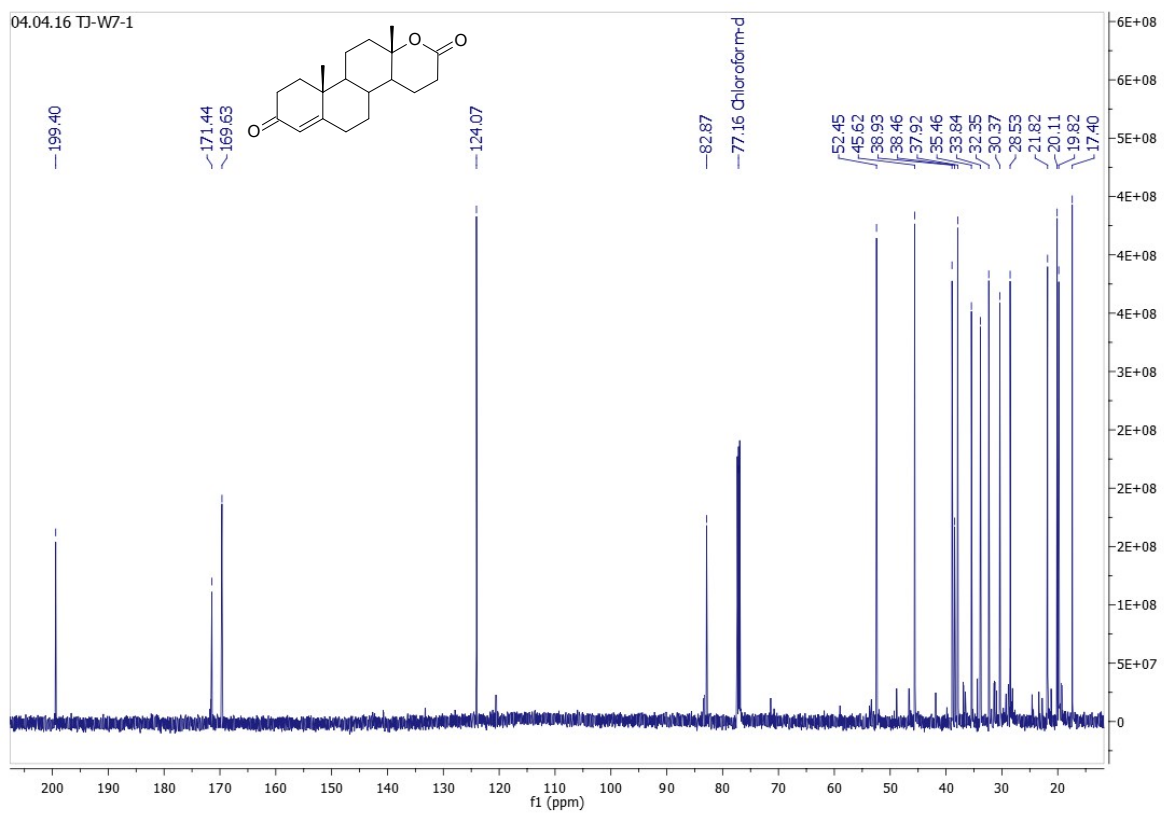


Fig.S19. HSQC spectral of 17a-oxa-D-homo-androst-4-ene-17-one (**testololactone**) ( $\text{CDCl}_3$ , 151 MHz)

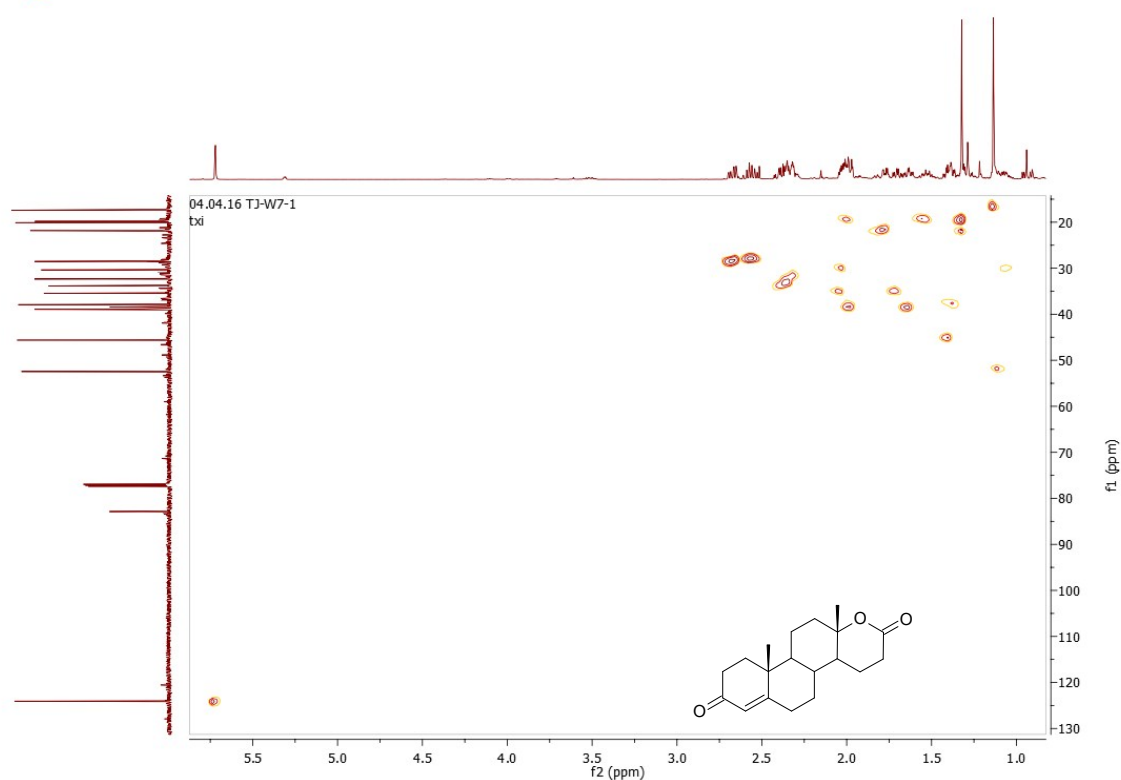


Fig.S20. COSY spectral of 17a-oxa-D-homo-androst-4-ene-17-one (**testololactone**) ( $\text{CDCl}_3$ , 151 MHz)

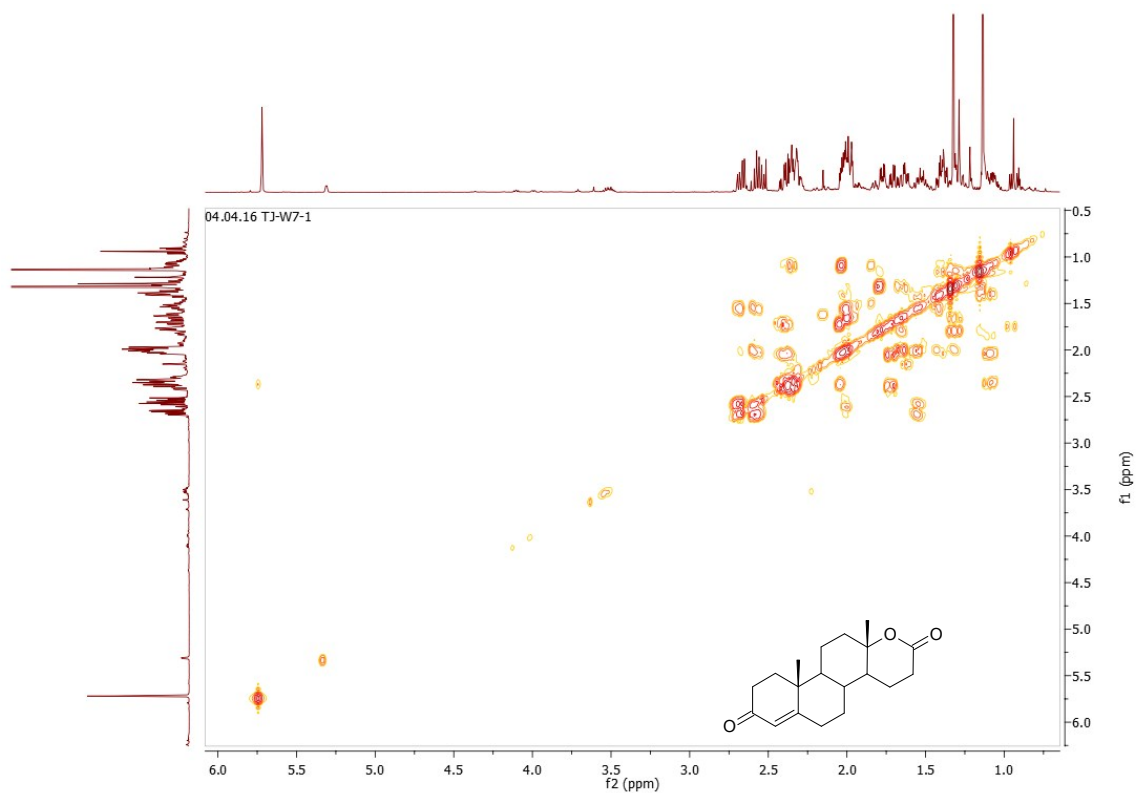


Fig.S21.  $^1\text{H}$  NMR spectral of  $3\beta,7\alpha$ -dihydroxyandrost-5-ene-17-one (**7 $\alpha$ OH-DHEA**) ( $\text{CDCl}_3$ , 600 MHz)

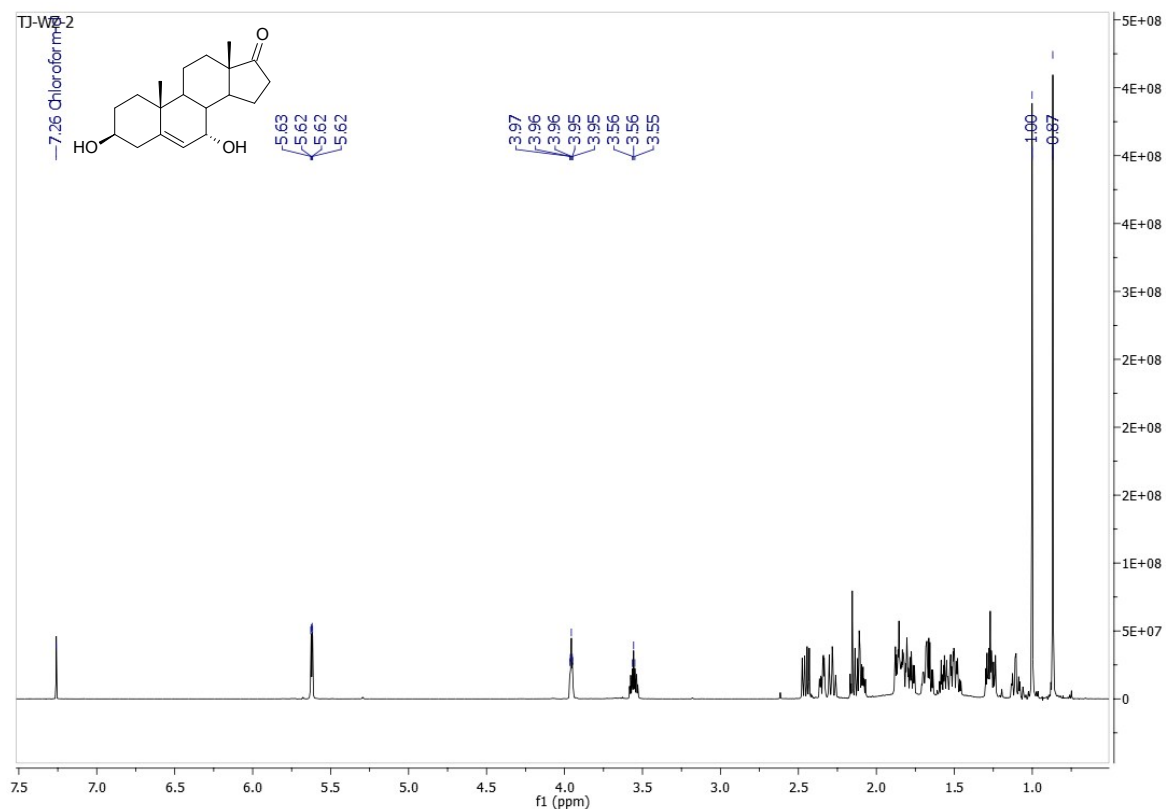


Fig.S22.  $^{13}\text{C}$  NMR spectral of  $3\beta,7\alpha$ -dihydroxyandrost-5-ene-17-one (**7 $\alpha$ OH-DHEA**) ( $\text{CDCl}_3$ , 151 MHz)

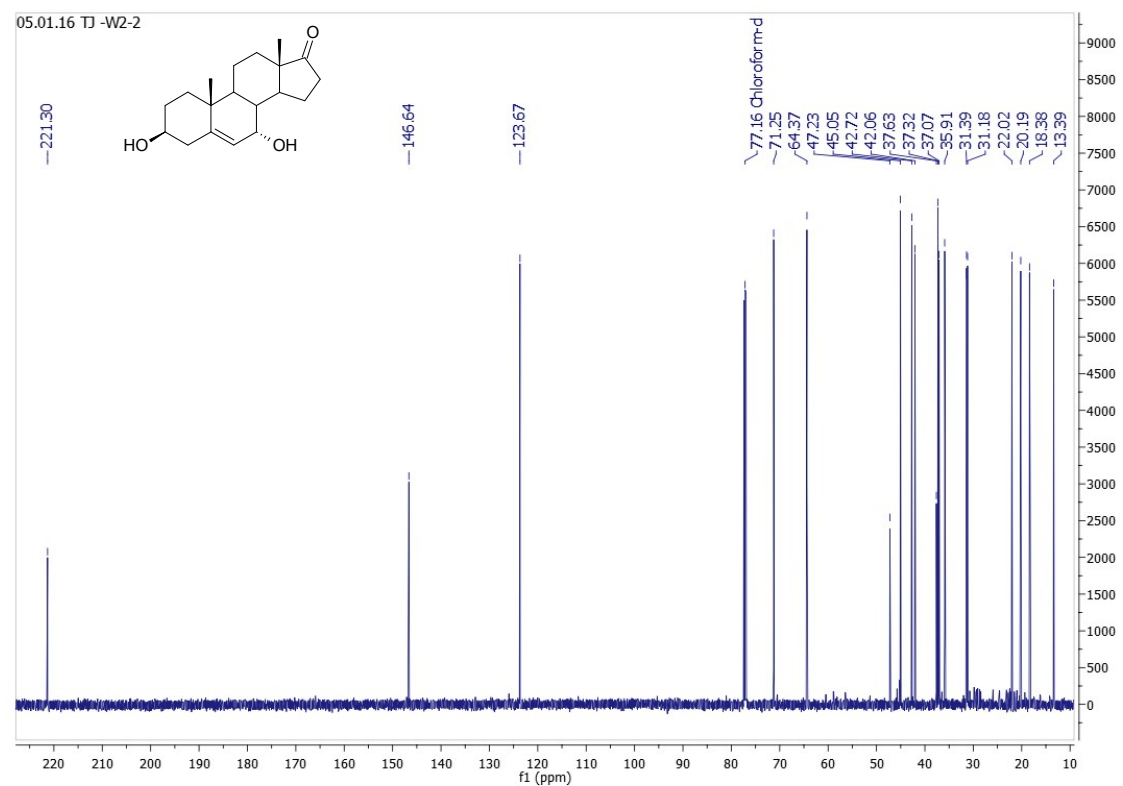


Fig.S23. HSQC spectral of  $3\beta,7\alpha$ -dihydroxyandrostan-5-ene-17-one (**7 $\alpha$ OH-DHEA**) ( $\text{CDCl}_3$ , 151 MHz)

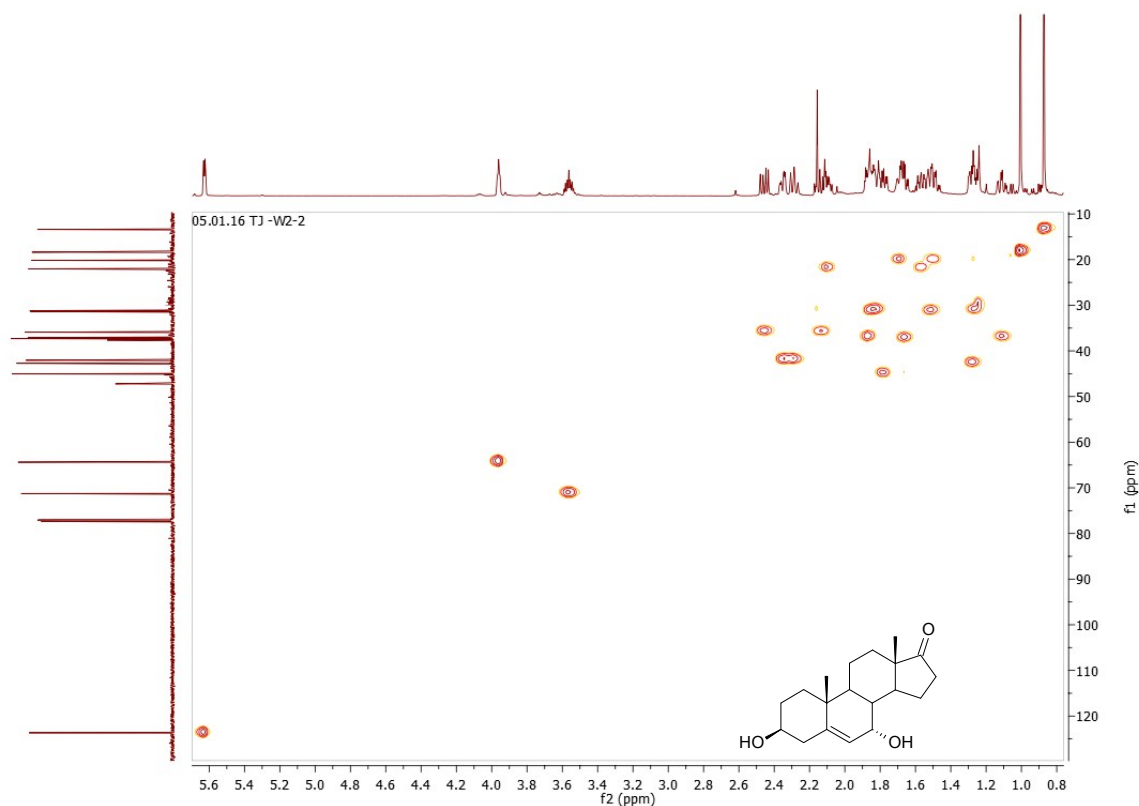


Fig.S24. COSY spectral of  $3\beta,7\alpha$ -dihydroxyandrostan-5-ene-17-one (**7 $\alpha$ OH-DHEA**) ( $\text{CDCl}_3$ , 151 MHz)

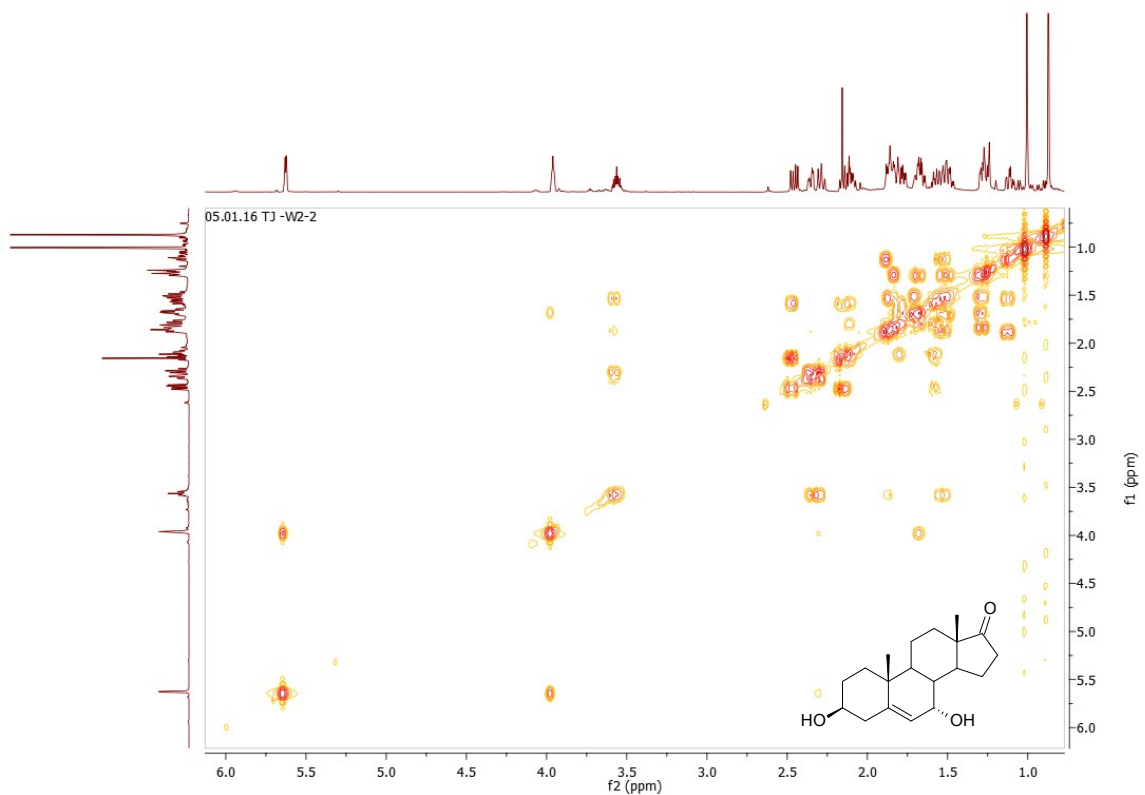


Fig.S25.  $^1\text{H}$  NMR spectral of androst-5-ene-3 $\beta$ ,7 $\alpha$ ,17 $\alpha$ -triol (**3 $\beta$ ,7 $\alpha$ ,17 $\alpha$ -triol**) ( $\text{CDCl}_3$ , 600 MHz)

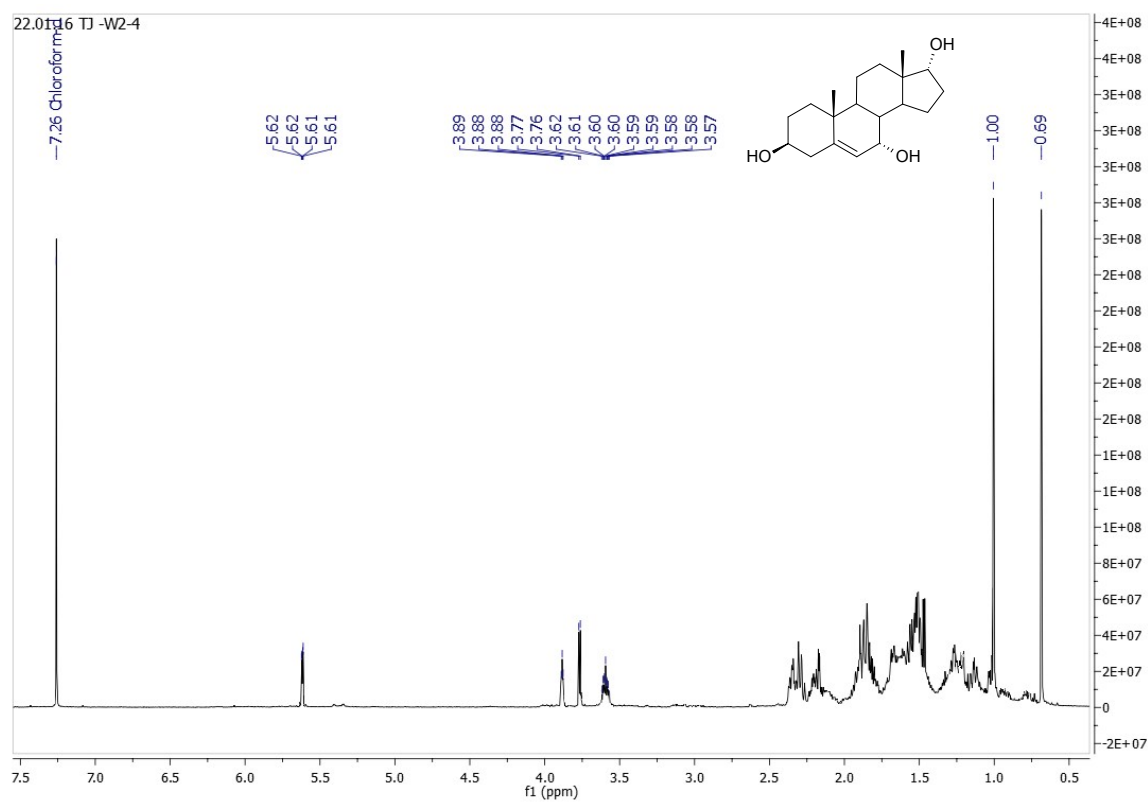


Fig.S26.  $^{13}\text{C}$  NMR spectral of androst-5-ene-3 $\beta$ ,7 $\alpha$ ,17 $\alpha$ -triol (**3 $\beta$ ,7 $\alpha$ ,17 $\alpha$ -triol**) ( $\text{CDCl}_3$ , 151 MHz)

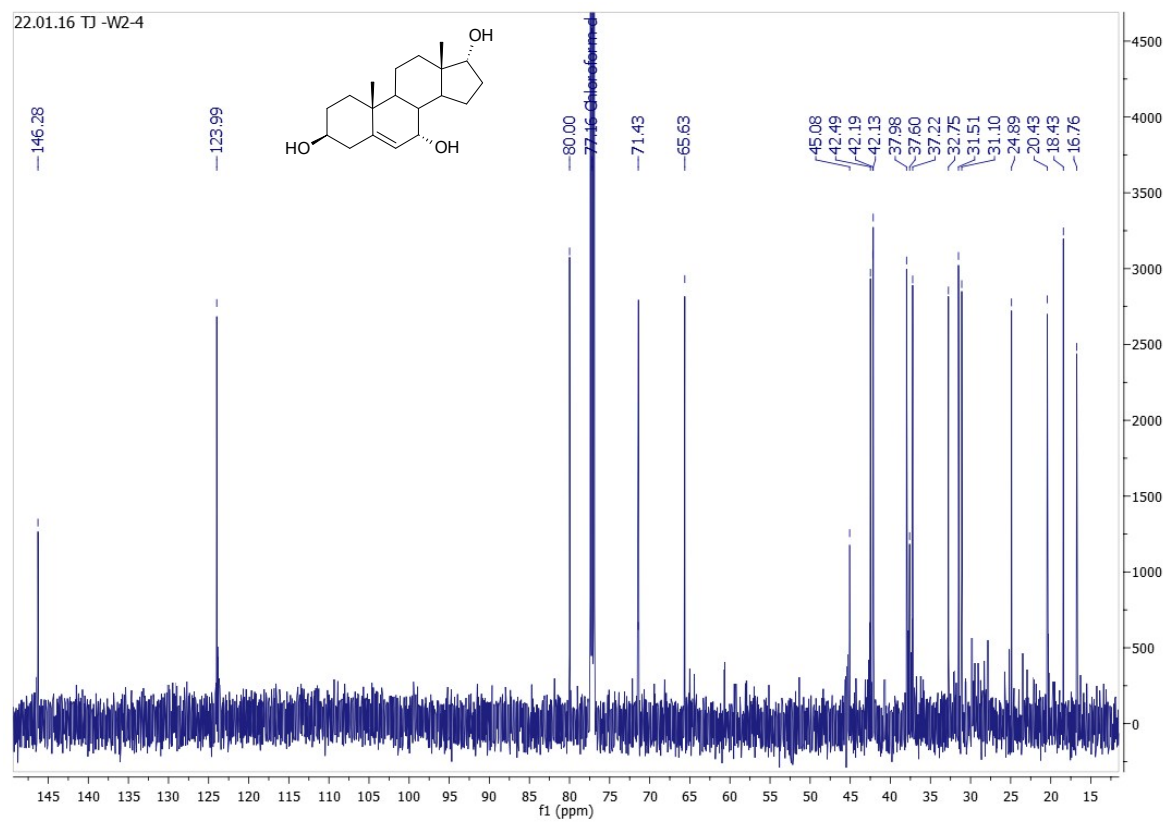


Fig.S27. HSQC spectral of androst-5-ene-3 $\beta$ ,7 $\alpha$ ,17 $\alpha$ -triol (**3 $\beta$ ,7 $\alpha$ ,17 $\alpha$ -triol**) ( $\text{CDCl}_3$ , 151 MHz)

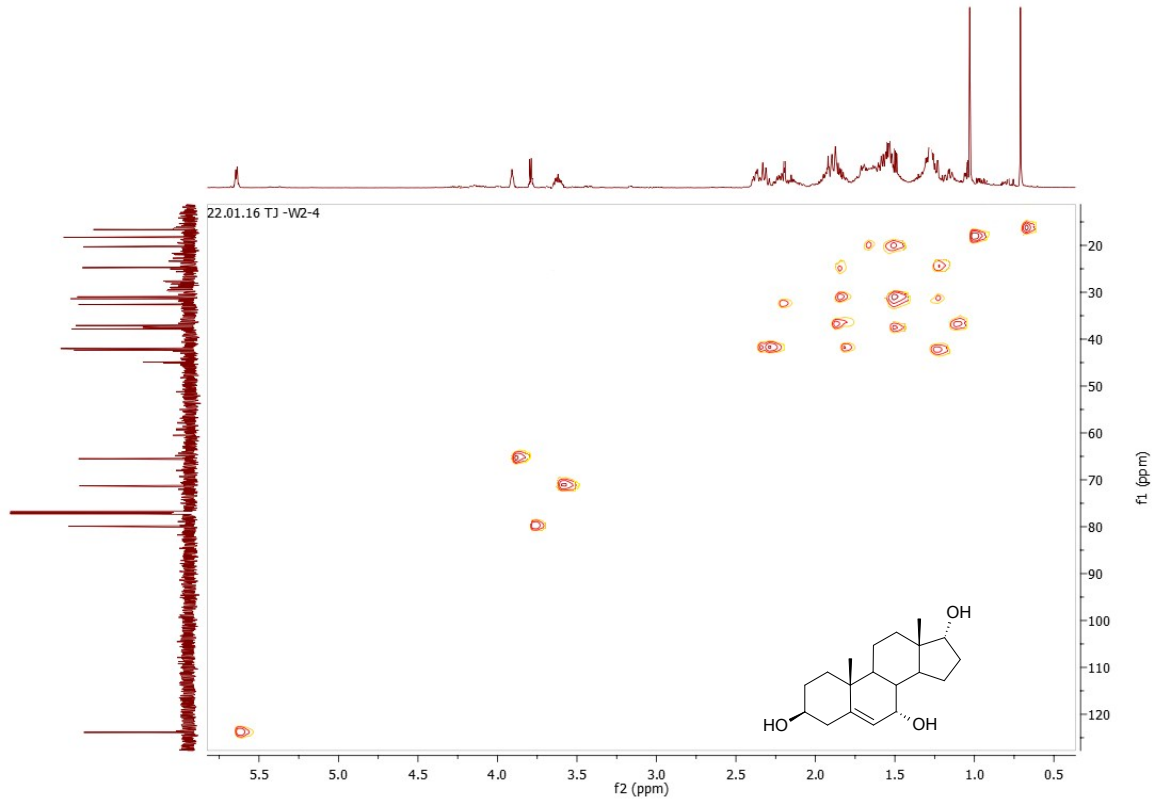


Fig.S28. COSY spectral of androst-5-ene-3 $\beta$ ,7 $\alpha$ ,17 $\alpha$ -triol (**3 $\beta$ ,7 $\alpha$ ,17 $\alpha$ -triol**) (CDCl<sub>3</sub>, 151 MHz)

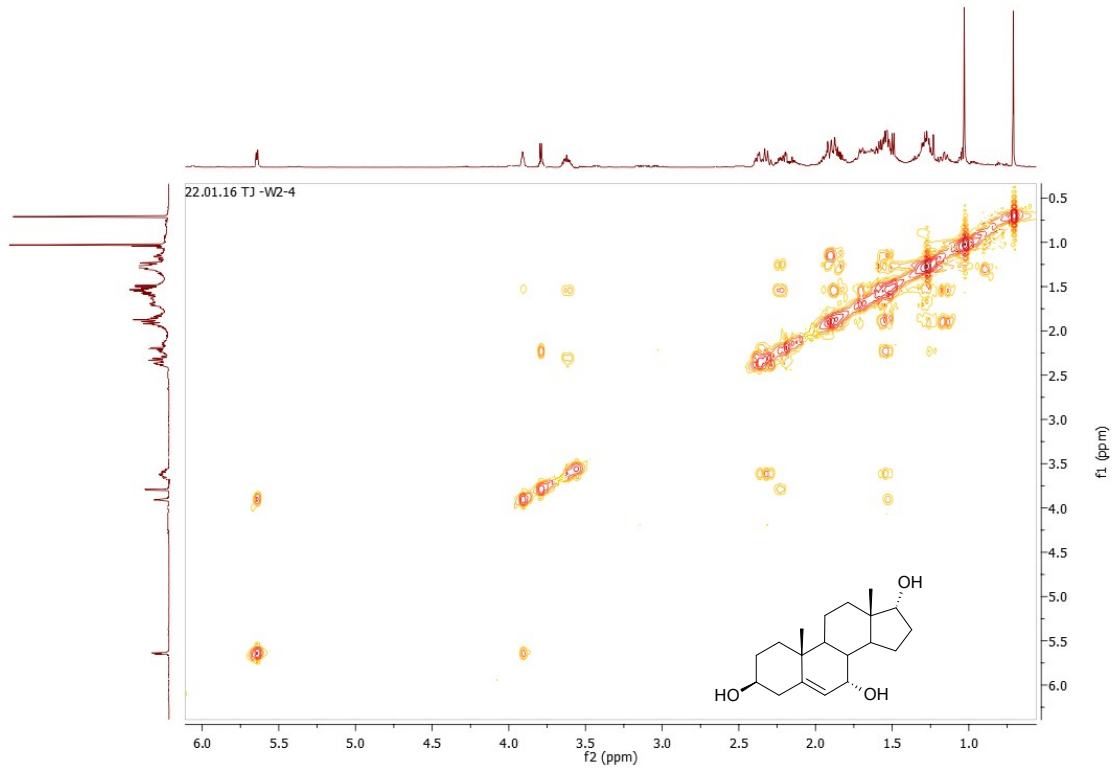


Fig.S29.  $^1\text{H}$  NMR spectral of 3 $\beta$ -hydroxyandrost-5-ene-7,17-dione (**7Oxo-DHEA**) ( $\text{CDCl}_3$ , 600 MHz)

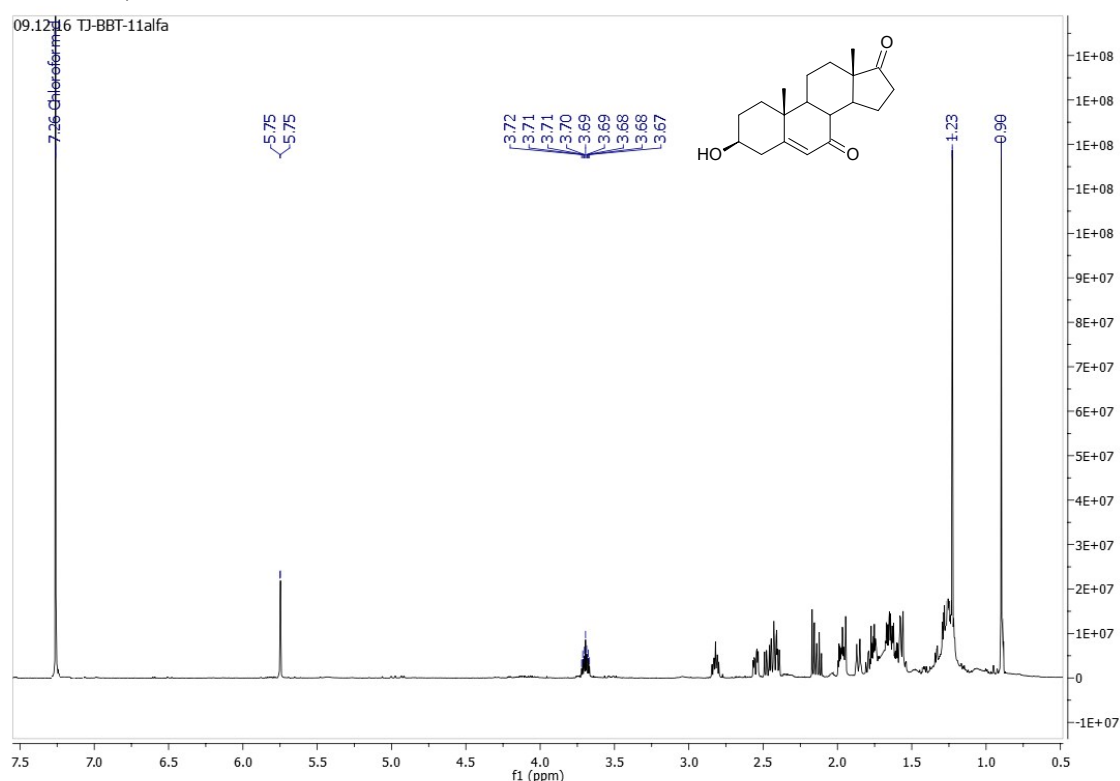


Fig.S30.  $^{13}\text{C}$  NMR spectral of 3 $\beta$ -hydroxyandrost-5-ene-7,17-dione (**7Oxo-DHEA**) ( $\text{CDCl}_3$ , 151 MHz)

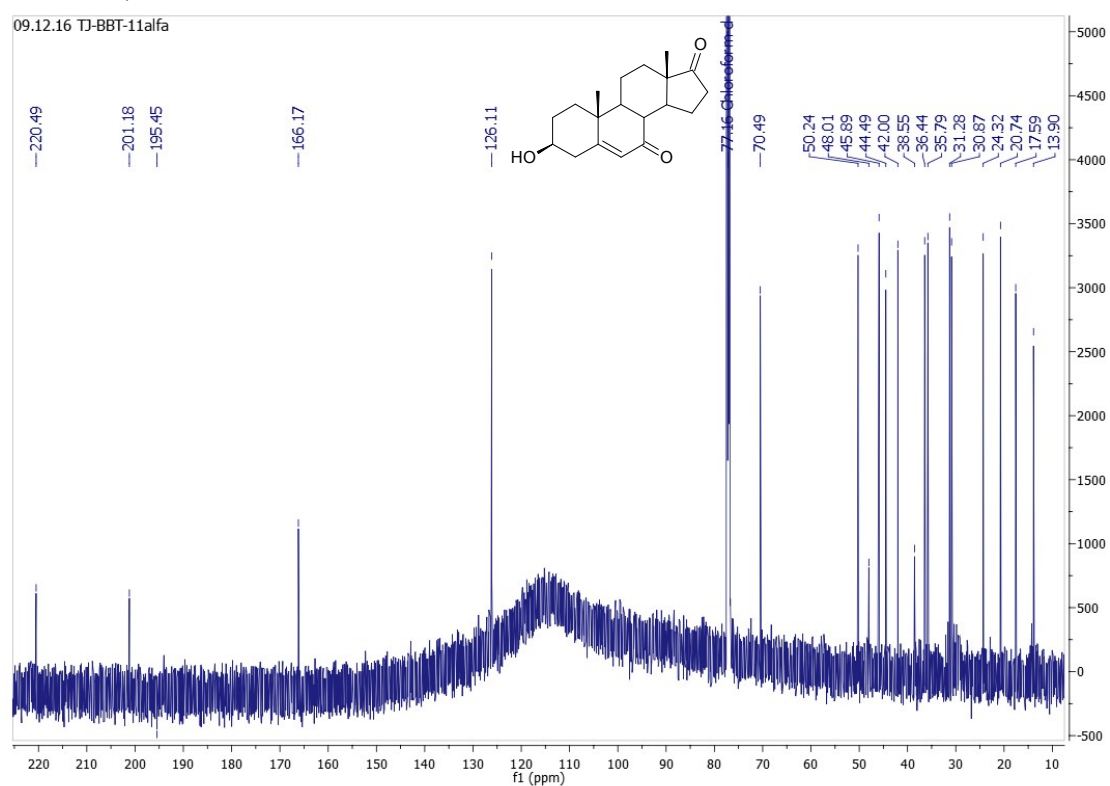


Fig.S31. HSQC spectral of 3 $\beta$ -hydroxyandrost-5-ene-7,17-dione (**7Oxo-DHEA**) ( $\text{CDCl}_3$ , 151 MHz)

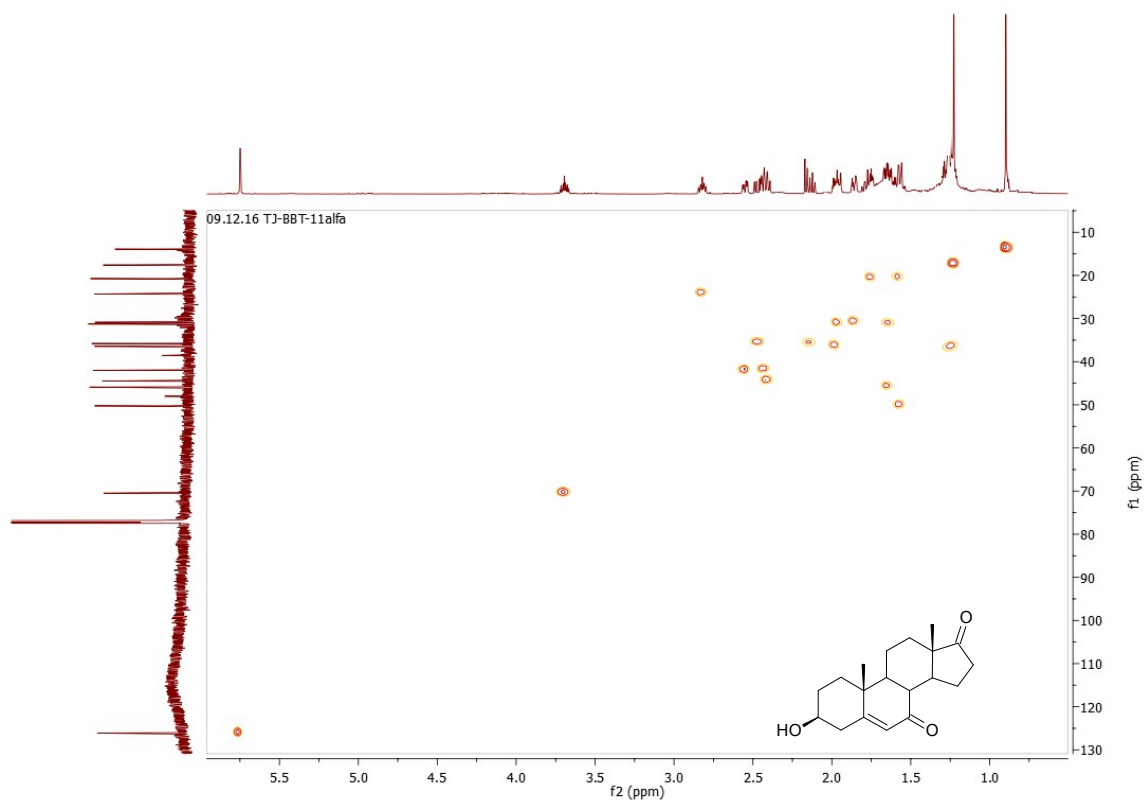


Fig.S32. COSY spectral of 3 $\beta$ -hydroxyandrost-5-ene-7,17-dione (**7Oxo-DHEA**) ( $\text{CDCl}_3$ , 151 MHz)

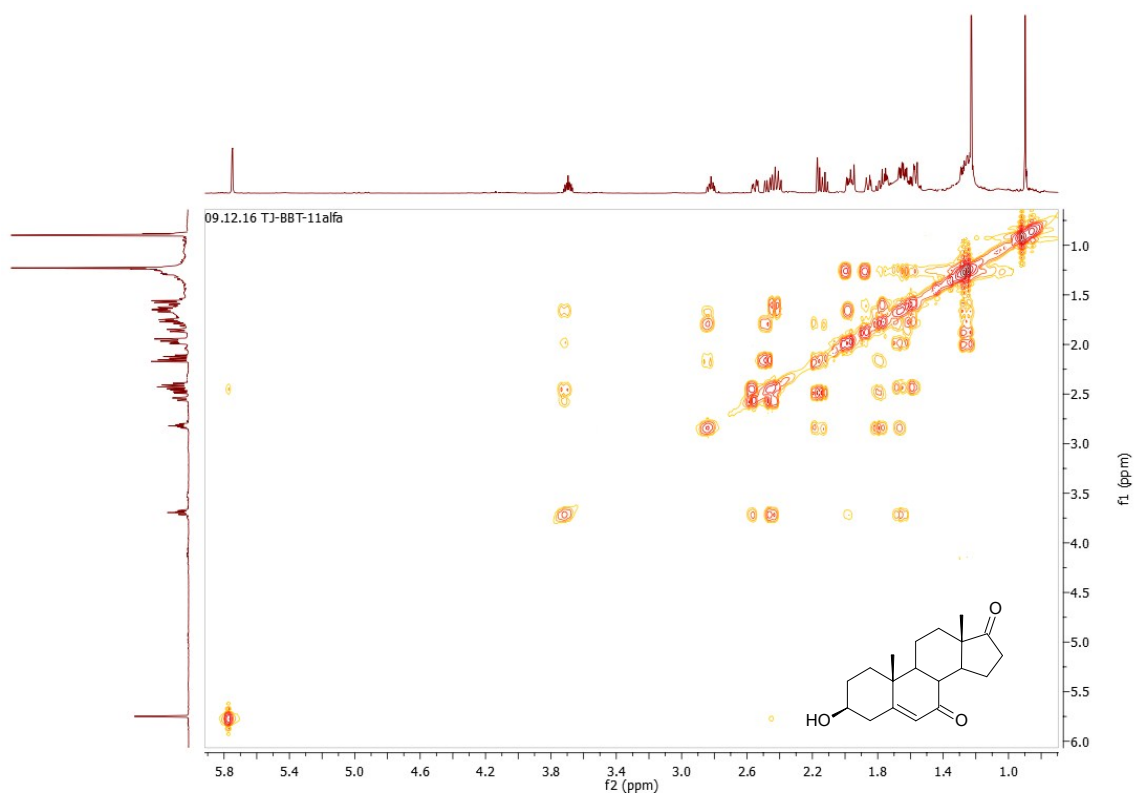


Table S2. Intensity of fragments arising from degradation of compound androst-1,4-diene-3,17-dione (**ADD**)

nr	Precursor ion ( <i>m/z</i> )	relative abundance [%]
1	122,10	100,00
2	121,10	14,91
3	91,05	11,94
4	107,05	10,99
5	159,05	10,64
6	123,10	9,30
7	93,05	7,98
8	79,05	7,57
9	108,10	7,31
10	105,10	6,48

Formula Weight = 284.39266  
Molecular Formula C<sub>19</sub>H<sub>24</sub>O<sub>2</sub>

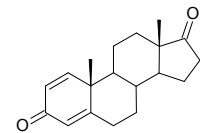


Fig.S33. GC-MS spectra of androst-1,4-diene-3,17-dione (**ADD**)

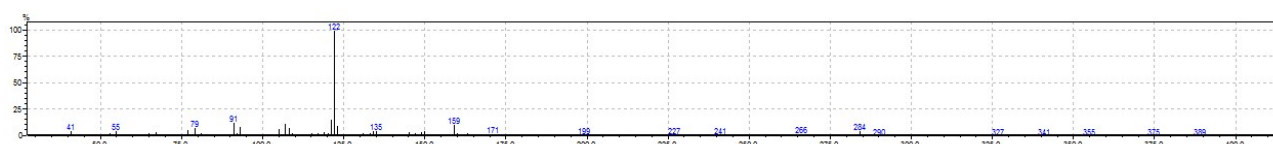


Fig.S34. Enlarged GC-MS spectra of androst-1,4-diene-3,17-dione (**ADD**)

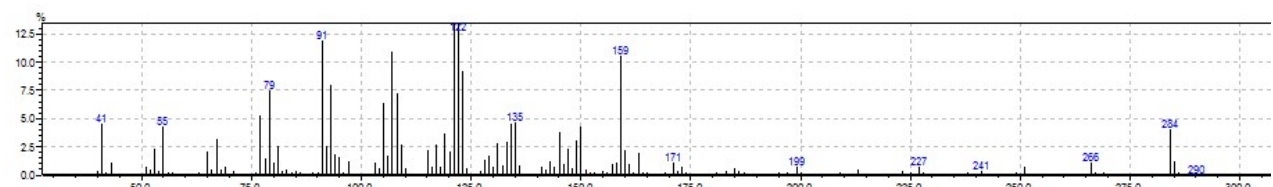


Table S3. Intensity of fragments arising from degradation of compound 6 $\beta$ -hydroxyandrost-4-ene-3,17-dione (**6 $\beta$ OH-AD**)

nr	Precursor ion ( $m/z$ )	relative abundance [%]
1	302,10	100
2	152,00	55
3	287,05	54
4	110,10	32
5	79,05	26
6	55,00	23
7	91,05	23
8	93,05	22
9	303,10	21
10	149,05	19

Formula Weight = 302.40794  
Molecular Formula C<sub>19</sub>H<sub>26</sub>O<sub>3</sub>

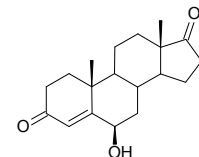


Fig.S35. GC-MS spectra of 6 $\beta$ -hydroxyandrost-4-ene-3,17-dione (**6 $\beta$ OH-AD**)

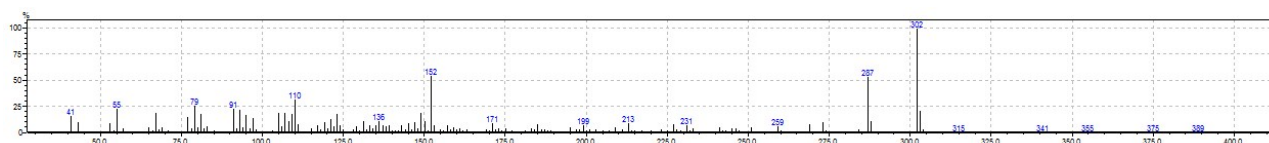


Fig.S36. Enlarged GC-MS spectra of 6 $\beta$ -hydroxyandrost-4-ene-3,17-dione (**6 $\beta$ OH-AD**)

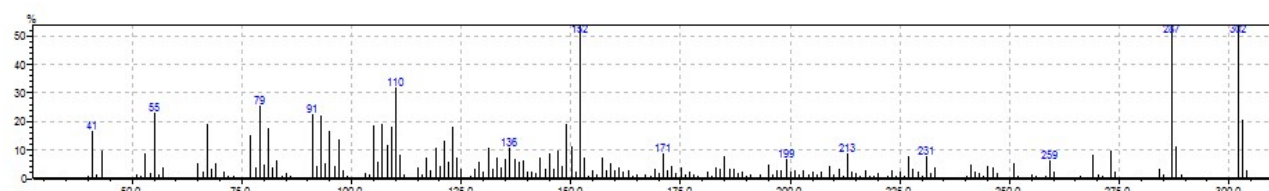


Table S4. Intensity of fragments arising from degradation of compound 6 $\beta$ -hydroxyandrost-1,4-diene-3,17-dione (**6 $\beta$ OH-ADD**)

nr	Precursor ion ( $m/z$ )	relative abundance [%]
1	121,10	100
2	134,10	69
3	119,10	50
4	91,05	46
5	133,10	46
6	122,10	44
7	105,10	33
8	147,05	31
9	123,10	28
10	77,05	29

Formula Weight = 300.39206  
Molecular Formula C<sub>19</sub>H<sub>24</sub>O<sub>3</sub>

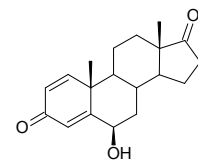


Fig.S37. GC-MS spectra of 6 $\beta$ -hydroxyandrost-1,4-diene-3,17-dione (**6 $\beta$ OH-ADD**)

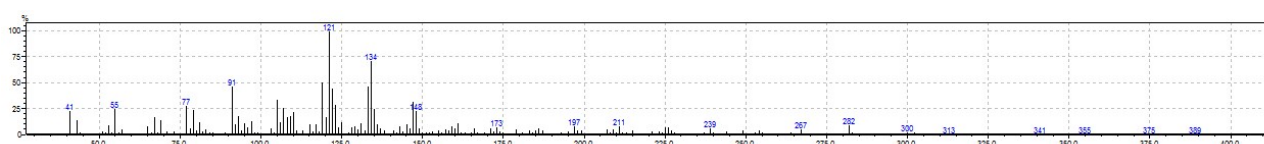


Fig.S38. Enlarged GC-MS spectra of 6 $\beta$ -hydroxyandrost-1,4-diene-3,17-dione (**6 $\beta$ OH-ADD**)

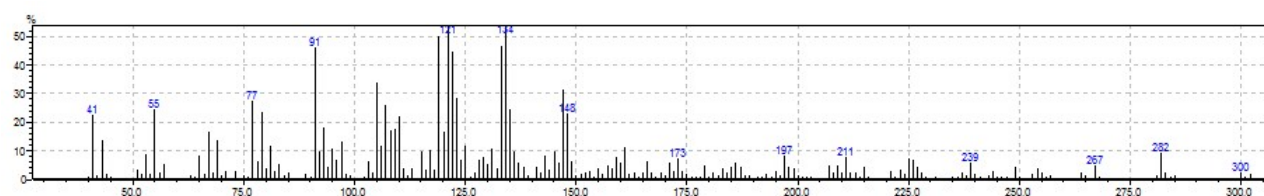


Table S5. Intensity of fragments arising from degradation of compound 3 $\beta$ -hydroxy-17a-oxa-D-homo-androst-5-ene-17-one (**3 $\beta$ OH-lactone**)

nr	Precursor ion ( $m/z$ )	relative abundance [%]
1	289,10	100
2	55,00	47
3	43,00	42
4	79,05	35
5	108,10	34
6	93,10	32
7	109,10	32
8	246,05	29
9	231,05	29
10	67,05	26

Formula Weight = 304.42382  
Molecular Formula C<sub>19</sub>H<sub>28</sub>O<sub>3</sub>

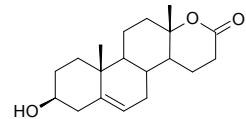


Fig.S39. GC-MS spectra of 3 $\beta$ -hydroxy-17a-oxa-D-homo-androst-5-ene-17-one (**3 $\beta$ OH-lactone**)

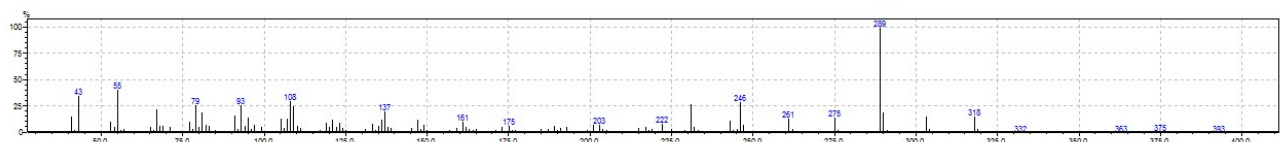


Fig.S40. Enlarged GC-MS spectra of 3 $\beta$ -hydroxy-17a-oxa-D-homo-androst-5-ene-17-one (**3 $\beta$ OH-lactone**)

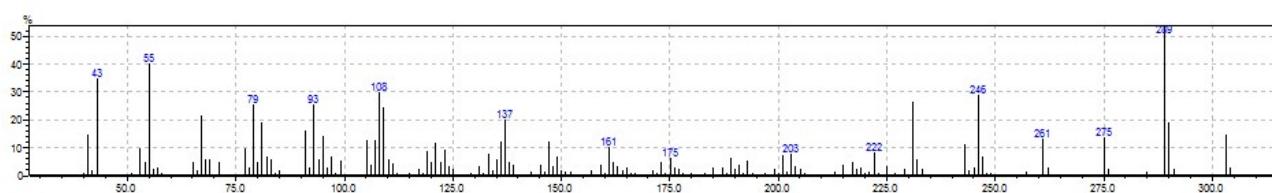


Table S6. Intensity of fragments arising from degradation of compound 17a-oxa-D-homo-androst-4-ene-17-one (**testololactone**)

nr	Precursor ion ( <i>m/z</i> )	relative abundance [%]
1	260,10	100
2	107,10	44
3	43,00	40
4	302,10	38
5	79,05	36
6	91,05	35
7	55,00	33
8	123,10	29
9	124,10	28
10	109,10	28

Formula Weight = 302.40794  
Molecular Formula C<sub>19</sub>H<sub>26</sub>O<sub>3</sub>

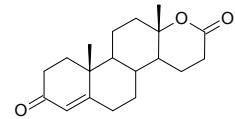


Fig.S41. GC-MS spectra of 17a-oxa-D-homo-androst-4-ene-17-one (**testololactone**)

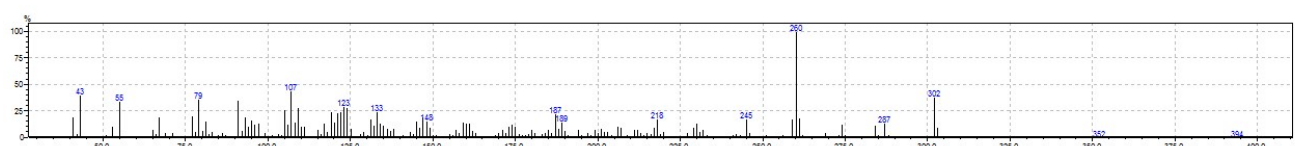


Fig.S42. Enlarged GC-MS spectra of 17a-oxa-D-homo-androst-4-ene-17-one (**testololactone**)

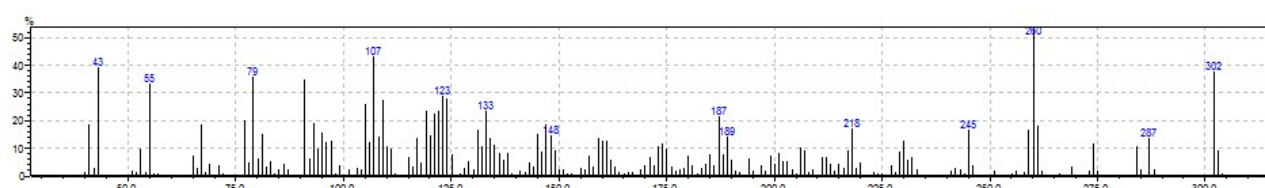


Table S7. Intensity of fragments arising from degradation of compound  $3\beta,7\alpha$ -dihydroxyandrost-5-ene-17-one (**7 $\alpha$ OH-DHEA**)

nr	Precursor ion ( $m/z$ )	relative abundance [%]
1	286	100
2	272	21
3	91	16
4	105	16
5	79	14
6	109	12
7	107	12
8	143	12
9	55	12
10	253	9

Formula Weight = 304.42382  
Molecular Formula C<sub>19</sub>H<sub>28</sub>O<sub>3</sub>

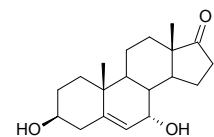


Fig.S43. GC-MS spectra of  $3\beta,7\alpha$ -dihydroxyandrost-5-ene-17-one (**7 $\alpha$ OH-DHEA**)

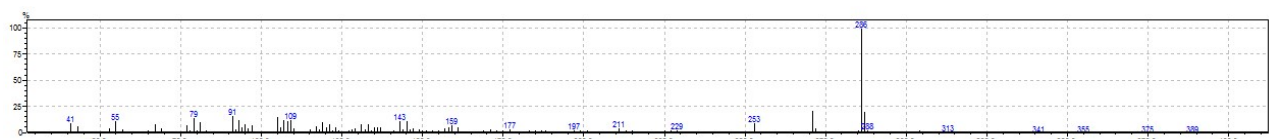


Fig.S44. Enlarged GC-MS spectra of  $3\beta,7\alpha$ -dihydroxyandrost-5-ene-17-one (**7 $\alpha$ OH-DHEA**)

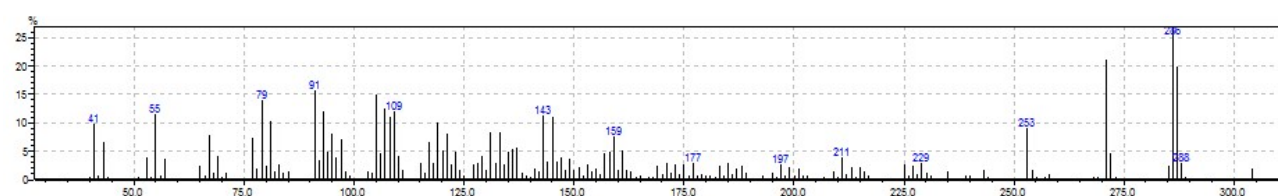


Table S8. Intensity of fragments arising from degradation of compound androst-5-ene-  
**3 $\beta$ ,7 $\alpha$ ,17 $\alpha$ -triol (3 $\beta$ ,7 $\alpha$ ,17 $\alpha$ -triol)**

nr	Precursor ion ( <i>m/z</i> )	relative abundance [%]
1	286	100
2	91	33
3	271	31
4	79	25
5	105	23
6	287	22
7	143	20
8	77	20
9	253	16
10	131	15

Formula Weight = 306.4397  
Molecular Formula C<sub>19</sub>H<sub>30</sub>O<sub>3</sub>

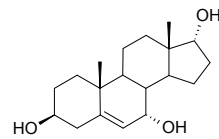


Fig.S45. GC-MS spectra of androst-5-ene-3 $\beta$ ,7 $\alpha$ ,17 $\alpha$ -triol (3 $\beta$ ,7 $\alpha$ ,17 $\alpha$ -triol)

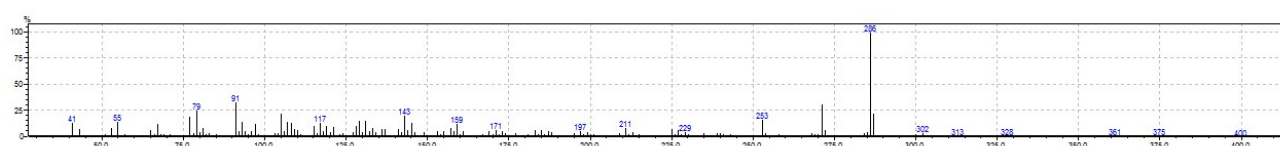


Fig.S46. Enlarged GC-MS spectra of androst-5-ene-3 $\beta$ ,7 $\alpha$ ,17 $\alpha$ -triol (3 $\beta$ ,7 $\alpha$ ,17 $\alpha$ -triol)

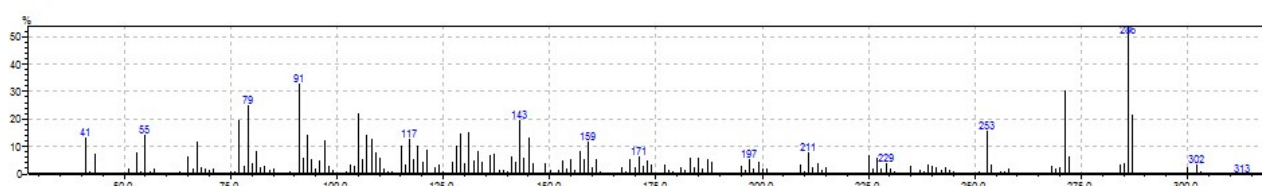


Table S9. Intensity of fragments arising from degradation of compound 3 $\beta$ -hydroxyandrost-5-ene-7,17-dione (**7Oxo-DHEA**)

nr	Precursor ion ( $m/z$ )	relative abundance [%]
1	91	100
2	161	94
3	134	93
4	284	90
5	241	74
6	229	60
7	187	59
8	256	57
9	119	54
10	105	49

Formula Weight = 302.40794  
Molecular Formula C<sub>19</sub>H<sub>26</sub>O<sub>3</sub>

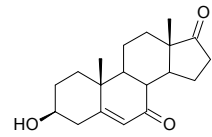


Fig.S47. GC-MS spectra of 3 $\beta$ -hydroxyandrost-5-ene-7,17-dione (**7Oxo-DHEA**)

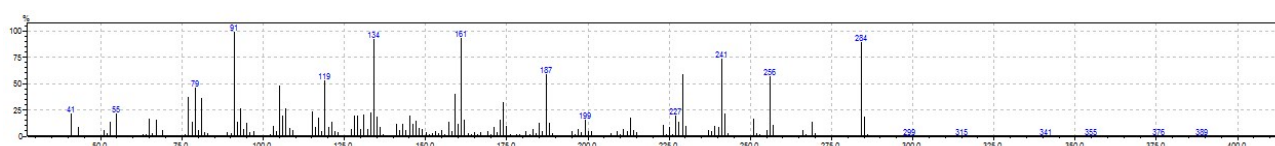


Fig.S48. Enlarged GC-MS spectra of 3 $\beta$ -hydroxyandrost-5-ene-7,17-dione (**7Oxo-DHEA**)

